

**ANALYSIS OF PORE PRESSURE AND SOIL MOVEMENT
OBSERVATION DATA OF RAREM DAM, NORTH LAMPUNG
INDONESIA**

A DISSERTATION

*submitted in partial fulfilment of the requirements
for the award of the degree*

of

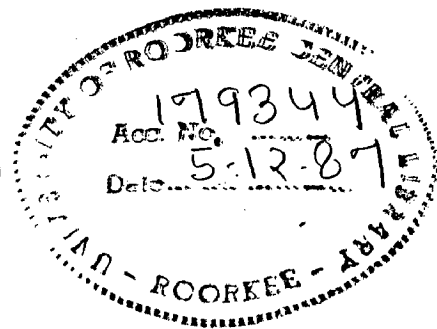
MASTER OF ENGINEERING

in

WATER RESOURCES DEVELOPMENT

By

DJOKO MUDJIHARDJO



**WATER RESOURCES DEVELOPMENT TRAINING CENTRE
UNIVERSITY OF ROORKEE
ROORKEE-247 667 (INDIA)**

November, 1986

C E R T I F I C A T E

Certified that the dissertation entitled, ' ANALYSIS OF PORE PRESSURE AND SOIL MOVEMENT OBSERVATION DATA OF RAREM DAM, NORTH LAMPUNG -INDONESIA' which is being submitted by Shri Djoko Mudjihardjo, in partial fulfilment of the requirement for the award of the degree of Master of Engineering in Water Resources Development of the University of Roorkee, is a record of the candidate's own work carried out by him under my guidance and supervision. The matter embodied in this dissertation has not been submitted for the award of any other degree or diploma to the best of my knowledge.

This is to further certify that Shri Djoko Mudjihardjo has worked for a period exceeding four months from July 16, 1986 for preparation of this dissertation.

R.P. Singh
(R.P. Singh)
Reader, WRDTC

ROORKEE

NOVEMBER 21, 1986

Dr. M.C. Goel
(Dr. M.C. Goel)
Professor
Water Resources Development
Training Centre
University of Roorkee
Roorkee, U.P.

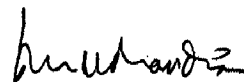
ACKNOWLEDGEMENT

I express my deep grateful to Dr. M.C. Goel, Professor, Water Resources Development Training Centre, University of Roorkee for his continuity guidance and encouragement during preparation of this dissertation. My sincere thanks is also addressed to Shri R.P. Singh, Reader, WRDTC for his assistance for preparing this work.

I am also very much grateful to Dr. A.S. Chawla, Professor and Head, WRDTC, University of Roorkee for extending the facilities for this work.

My deep grateful is also addressed to Director, Institute of Hydraulic Engineering and Head of Hydraulic Structures Division and his staffs (that it is impossible to thank them individually here), Ministry of Public Work, Government of Indonesia for their continuity encouragement.

Finally, for technical assistance and sympathetic forbearance during preparation of the laboratory experimental work, I owe debt to Shri R.S. Sharma and his staff.



(DJOKO MUDJIHARDJO)

ROORKEE

NOVEMBER 21 , 1986

TABLE OF CONTENTS

	Page
CERTIFICATE	
ACKNOWLEDGEMENT	
SYNOPSIS	
CHAPTER-1	INTRODUCTION ... 1
1.1	Definition of Pore Water Pressure ... 1
1.2	Various Types of Pore Pressures ... 4
1.2.1	End of Construction condition ... 5
1.2.2	Steady Seepage Pore Pressures ... 11
1.2.3	Draw Down pore pressure ... 13
1.3	Scope of Problems ... 19
CHAPTER-2	DESCRIPTION OF RAREM DAM ... 21
2.1	General Features ... 21
2.2	Geology of Dam Site ... 21
2.3	Dam Section ... 25
2.4	Material Properties ... 26
2.5	Foundation Treatment ... 30
2.6	Instrumentation ... 30
2.6.1	Necessity ... 30
2.6.2	Piezometers ... 32
2.6.3	Inclinometer/Magnetic Extensometer ... 37
2.6.4	Surface Monuments ... 38
2.7	Quality Control & Monitoring ... 40
2.7.1	Quality Control ... 40
2.7.2	Monitoring ... 42
CHAPTER-3	PRESENTATION & ANALYSIS OF OBSERVATIONAL DATA ... 43
3.1	Pore Pressures ... 43
3.1.1	Presentation of Observational Data ... 43
3.1.2	Analysis of Pore Pressures Data ... 45
3.2	Vertical & horizontal movement ... 68
3.2.1	Vertical movement (Settlement) ... 68
3.2.2	Horizontal Movement ... 72

Contd.

Table of Contents(contd.)		Page
CHAPTER-4	EXPERIMENTAL SET-UP	... 77
	4.1 General	... 77
	4.2 Analog Approach	... 78
	4.3 Conductive tray method	... 80
	4.3.1 Model	... 80
	4.3.2 Electrolytes	... 82
	4.3.3 Instrumental set-up	... 83
CHAPTER-5	COMPARISON AND ANALYSIS OF OBSERVED AND LABORATORY TEST DATA	... 89
	5.1 Cases Studied	... 89
	5.2 Presentation of Experimental Data	... 89
	5.3 Comparison and Analysis	... 90
CHAPTER-6	CONCLUSION	... 107
	REFERENCES	... 111

S Y N O P S I S

28 m high Rarem dam was completed in Indonesia on October 1983. It is a zoned section comprising vertical clay core of high plasticity and rock shells as resting on permeable tuff rock foundation consolidation and curtain grouting have been provided as foundation treatment due to perviousness of foundation layers. Reservoir filling was started immediately after construction was over in three months time. Till then, there has been no drawdown.

The instrumentation on Rarem Dam consists of pore pressures measuring downs and vertical and horizontal displacement measuring devices. Observations on all instruments were carried out from their date of installation till end of December 1985 except a brief break of 2-3 months.

The study of observational data has indicated that vertical settlement coincided with construction period and reservoir filling and subsequent settlements are negligibly small. The overall settlement is of their order of 1% out of which 1/3rd has taken place during construction period itself. Very low construction pore pressures (25%) are recorded. Free surface line has fully developed simultaneously with reservoir filling and there is no time lag in pore pressure development.

In order to judge the efficacy of grouting model studies based electrical analogy simulating consolidation zone and foundation permeabilities were carried out in conductive tray. The studies have indicated that grouting is successful in this project.

1. INTRODUCTION

1.1 Definition of Pore Water Pressure

Partially saturated soils have three phase composition, viz. solids, water and air. These three phases can reduce to two as in case of phases viz. solid state and pore air are present whereas in fully saturated soil only soil particles and pore water are present. When load is applied to a soil mass, part is carried by the mineral skeleton and part by the pore fluid, the load being distributed in direct proportion to the relative stiffness of the phases. If the pore space is filled by air and water, the load is supported by the water(and air) at the beginning and as time passes on, the load is gradually transferred to the soil skeleton. The pressure which is supported by water is called pore water pressure and more commonly known as pore pressure.

For fully saturated soils, it was shown by Terzaghi (1923) that the effective stress

$$\sigma' = \sigma - u_w \quad (1.1)$$

where u_w is pore water pressure, σ is total stress and σ' is effective stress.

Skempton (1960) also confirmed that the total force is

$$\sigma.A = \sigma'.A + u_w(1-a) A \quad (1.2)$$

where,

A = area of an element of soil

a = the fraction of cross-sectional area that is occupied by the points of contact of the soil grains. The force from the pore water pressure acts over an area $(1-a)A$.

According to Bishop and Edin (1950), the value of 'a' is very small and may be ignored to give -

$$\sigma' = \sigma - u_w \quad (1.1)$$

At any point the pore water pressure u_w , acts equally in all directions causing hydrostatic compression of the soil particles, but this could be ignored, because the compressibility of the soil particle itself is very large.

The pore water pressure u which represents the effects of the pore air, u_a and pore water u_w is -

$$u = u_a - X (u_a - u_w) \quad (1.3)$$

In fully saturated soil, $X = 1.0$ and in a perfectly dry soil $X = 0$ (Croney et.al., 1958 and Bishop et.al., 1961) and varies in partly saturated soil, depend on degree of saturation.

Again Skempton (1954) derived the expression

$$\Delta u = B \left[\Delta \sigma_3 + A(\Delta \sigma_1 - \Delta \sigma_3) \right] \quad (1.4)$$

where,

Δu = Change in pore water pressure due to stress changes of $\Delta \sigma_1$ and $\Delta \sigma_3$ acting on element

A and B = dimensionless parameters.

Bishop and Henkel (1962) determined the values of A and B in the laboratory and the field measurement of pore water pressure in earth structures has shown the closed relationship between both parameters measured from laboratory and field (Lambe 1962, Bishop and Bjerrum, 1960).

Bishop rearranged Skempton's expression as -

$$\frac{\Delta u}{\Delta \sigma_1} = \bar{B} = B \left\{ 1 - (1-A) \left(1 - \frac{\Delta \sigma_3}{\Delta \sigma_1} \right) \right\} \quad (1.5)$$

where \bar{B} derived as pore pressure ratio, gives the change in pore pressure due to stress change under undrained conditions. The actual pore pressure also depends on the initial value, u_0 before the stress change is made and given as

$$u = u_0 + \Delta u = u_0 + \bar{B} \Delta \sigma_1 \quad (1.6)$$

In the case of no dissipation of pore pressure, the pore pressure ratio will be -

$$r_u = \frac{u}{\gamma h} = \frac{1}{\gamma h} (u_o + \bar{B} \Delta\sigma_1) \quad (1.7)$$

In the case of construction of earth dams, average value of $\Delta\sigma_1$ along a potential slip surface is approximated by γh and the equation becomes -

$$r_u = \bar{B} + \frac{u_o}{\gamma h} \quad (1.8)$$

For earth fills of low plasticity material placed wet of optimum moisture content such that the value of \bar{B} is high, the term of $u_o/\gamma h$ might be omitted to give

$$r_u = \bar{B} \quad (1.9)$$

This term is applied for calculating the slope stability in preliminary design.

1.2 Various Types of Pore Pressures

The shearing strength of fill material mobilized in earth dam depends on the magnitude of pore pressures occurring on any soil element. The pore water pressures have a dominant influence on the safety factor of the slope stability by reducing the shear parameters of soil.

Accordingly there are three conditions in a dam, where the pore pressures might effect -

- a) End of construction
- b) Steady seepage at full reservoir level
- c) Rapid draw down

In an earth dam, installation of a piezometer system coupled with settlement observation device is advantageous for actual measurements under prototype conditions and comparing these values with predicted values used in design. Remedial action can then be taken excessive pore pressures are recorded and the safety of dam is endangered. Similarly, non-uniform deformation could result in the development of cracks in which case prompt remedial action would be essential.

1.2.1 End of construction condition

The development of pore pressure during construction depend on many factors which the designer can not evaluate well in advance such as the influence of the weather to the moisture content (placement of moisture content), the rate of construction, moisture density control, soil type, drainages etc.

There are two common ways for estimating the construction of pore pressure from laboratory tests -

- a) Direct measurement of pore pressures on laboratory specimens which have been compacted at water content and densities expected during construction and which are then subjected to increasing stresses with a test procedure designed to simulate the stresses anticipated on the various elements of the embankment by the added weight of the overlying material during construction.

The determination of pore pressures in laboratory have been studied by Bishop and Henkel (1957) and also by some modification made by Govind Rao and Balakrishna (1961) to overcome the problems in de-airing system of Bishop type device.

- b) Hilf's method, by using conventional one-D consolidation test to determine the compression characteristic of the partially saturated embankment material. By assuming that the pressure in the pore water and pore air are equal and no dissipation of pore pressure occurs, decrease in embankment volume is caused by compression of air and its passing into solution in the pore water.

Applying Boyle's and Henry's law and equating product of pressure and volume of the pore air before and after embankment compression.

$$p_o(V_a + HV_w) = (p_o + u) (V_a + HV_w - \Delta)$$

Hence -
$$u = \frac{p_o \Delta}{V_a + HV_w - \Delta} \quad (1.10)$$

where,

u = induced pore air pressure

p_o = the absolute atmospheric pressure

Δ = embankment compression as a proportion of original embankment volume

V_a = Volume of free air in soil pores before start of consolidation in unit volume of the embankment soil.

V_w = Volume of pore water in unit volume of embankment soil.

HV_w = volume of dissolved air in volume V_w of water, where H is Henry's constant = 0.0198.

If the soil becomes saturated, $\Delta = V_a$, and pore pressure is given by -

$$u_{sat} = \frac{p_o \cdot V_a}{HV_w} \quad (1.11)$$

If

V_o = original volume of the soil mass

n_o = porosity

ΔV = volume change

S_o = initial degree of saturation

$$V_o n_o = \text{volume of voids}$$

$$V_o = (1-S_o)V_o n_o = \text{free air volume}$$

$$HS_o V_o n_o = \text{dissolved air}$$

$$\text{Hence, } V_a + HV_w = (1 - S_o + S_o H)V_o n_o \quad (1.12)$$

By noting that $\Delta = \frac{\Delta V}{V_o}$, and substituting $(V_a + HV_w)$ to the equation (1.10) -

$$u = \frac{-p_o \frac{\Delta V}{V_o}}{n_o(1-S_o + S_o H) + \frac{\Delta V}{V_o}} \quad (1.13)$$

is known as Bishop's relationship.

An approximate method of allowing for the various factors leading to pore pressure dissipation in the field has been developed by Bishop comprises step by step computation of pore pressure by Hilf's equation at certain stages of construction with intervals during which some pressure release is permitted. This procedure involves the effect of pore pressure dissipation during the shut-down period between construction season.

The computation of pore pressure in the fill during construction is done by assuming no drainage and then allowed pore pressure dissipation in a certain proportion before the application of the embankment loading from the next

construction season. The process is repeated to include the effect of various loading stages.

C.Y.Li (1959) has shown that the effect of drainage on the construction of pore pressures is cumulative and too great to be ignored. This effect of continuous dissipation can be accounted for by applying a dissipation factor defined as the ratio in which relief is permitted, at the end of each step of the computation.

The results obtained in the latter case can be joined by a continuous curve to obtain the pore pressure corresponding to the assumed value of dissipation factor. According to Li, even with an approximate value of dissipation factor, the calculated values of pore pressures are closer to the reality than those assuming no drainage.

R.E. Gibson described a method of allowing pore pressure dissipation concurrent with construction of the dam. This method is based on an analogy between the increase in the thickness of a clay layer with time and the increase in thickness of a sediment layer with time. The equation derived, was based on Terzaghi's consolidation theory describing the change in pore water pressure and change in effective stress -

$$C_v \frac{\partial^2 u_w}{\partial x^2} = \frac{\partial u_w}{\partial t} - \gamma \frac{dh}{dt} \quad (1.14)$$

where,

C_v	=	Coefficient of consolidation
u_w	=	pore water pressure
x	=	distance above the impermeable base
t	=	elapsed time
γ	=	unit weight of the material
h	=	current thickness of fill

By assuming the flow of pore water is vertical, the above equation is modified as

$$C_v \frac{\partial^2 u_w}{\partial x^2} = \frac{\partial u_w}{\partial t} - \gamma \bar{B} \frac{dh}{dt} \quad (1.15)$$

where \bar{B} = overall pore pressure coefficient = $\frac{\Delta u_w}{\Delta \sigma_1}$

The difficulty is that in construction of a dam, there is no initial starting point, since there is no initial layer. The analytical solution may be done by assuming the initial rate of thickening as constant.

Singh(1985) has utilized Goel's (1980) transient pore pressure two-dimensional mathematical model using plane-strain condition applicable to Biot's 3-D consolidation theory for predicting construction pore pressures during construction period.

Second order partial differential equation (1.16) in non-dimensional form governing pore pressure distribution during construction and seasonal shutdown has been solved for known boundary and initial condition using Finite Difference Method. However, his solution is not applicable to real world problem because of very large time interval adopted by him.

$$\frac{\partial^2 F}{\partial x^2} + \frac{\partial^2 F}{\partial x^2} = \frac{\partial F}{\partial t} - R_m \frac{\partial H_m}{\partial t} \quad (1.16)$$

where,

$$R_m = \frac{\gamma_m}{\gamma_w}$$

γ_m = Unit weight of fill material

γ_w = Unit weight of water

t = any time

F = pore pressures in non-dimensional form

H_m = dimensionless height of fill = h/h_o

h = height of dam at any consideration point

h_o = final height of dam.

2.2.2 Steady seepage pore pressures

The pore pressures which exist within an embankment are generated as the result of two actions which can be considered independent for practical purpose.

- a) Gravity seepage flow
- b) Changes in pore volume due to changes in total stresses.

The stability analysis on this condition is always using the effective stress method and the pore pressures acting are assumed to be those governed by gravity flow through embankment.

The shear strengths used should be those determined from consolidated - undrained test on saturated samples to which pore pressures are applied simulating those which may exist under the gravity flow in the dam and foundation.

The pore pressure distribution in the embankment due to gravity seepage is estimated from graphical flow nets or electrical analogy models.

The degree of anisotropy must be chosen adequately and the following values are conservative -

Sl. No.	Description of Soil in Borrow Area	$K_{hor}/K_{vert.}$
1.	Very uniform deposit of fine grained soil (CL and ML)	9
2.	Very uniform deposit of coarse soils with fines (GC and GH)	25
3.	Very erratic soils deposits	100 or higher

vertical filter drain is put at the axis of a dam.

b) Transient flow nets

The rate of dissipation of drawdown pore pressures can be roughly estimated by drawing a series of flow nets with a gradually lowering upper phreatic line.

An analytical method for determining the rate of of a saturation line following draw down was studied by Cedergren (1948). If V_{sl} is the rate of fall of saturation line and ΔL be the length of movement at any element in time Δt .

$$V_{sl} = \frac{\Delta L}{\Delta t} \quad (1.17)$$

By applying Darcy's law

$$V_{sl} = K \cdot i_o \cdot C_o \quad (1.18)$$

where,

K = Coefficient of permeability

i_o = hydraulic gradient

C_o = drainage factor given by

$$C_o = \frac{1+e}{e} \cdot \frac{W_w}{W_c} \quad (1.19)$$

- e = void ratio
 W_w = saturation water content
 W_c = change in water content caused by a change from the moist to the saturation state or vice versa.

c) Reinius' approach (1948)

By drawing flow nets for different u/s slope and different draw down reservoir levels, Reinius has shown that for semi pervious fill, the volume of water draining out from the pore space is large as compared to volume change induced by stress changes, the dissipation of pore pressure is a function of the parameter $K/n_s \cdot V_o$, where

- K = Coefficient of permeability
 n_s = specific yield
 V_o = rate of draw down

d) Cassagrande approximate theory

Cassagrande developed a simplified solution of the rate of drainage of the u/s shell of an earth dam. It is assumed that the upper phreatic line at various time following instantaneous drawdown may be approximated by inclined straight lines passing through the u/s toe.

$$T = \frac{u}{100+u} + J \log_e \frac{100}{100-u} + J^2 \frac{u}{100} \quad (1.20)$$

where,

u = percent - drainage

$$J = \frac{H}{L} \cot \beta \quad (\text{dimensionless}) \quad (1.21)$$

$$T = \frac{t \cdot K \cdot H}{n_s L^2} \quad (\text{dimensionless}) \quad (1.22)$$

if $\beta = 90^\circ$, the solution becomes simply

$$T = \frac{u}{100-4} \quad (1.23)$$

1.2.3.2 Compressible fill

In compressible fills which compress appreciably under draw down, the Laplacian equation would not be applicable.

Bishop has given the following equation for estimating draw down pore pressure

$$u = \gamma_w \left[h_c + h_r(1-\bar{B} n_s) + h_w(1-\bar{B}) - h' \right] \quad (1.24)$$

where,

u = pore pressure after draw down

h_c = height of impervious core

h_r = height of free draining material above the element

h_w = height of water column above the slope line

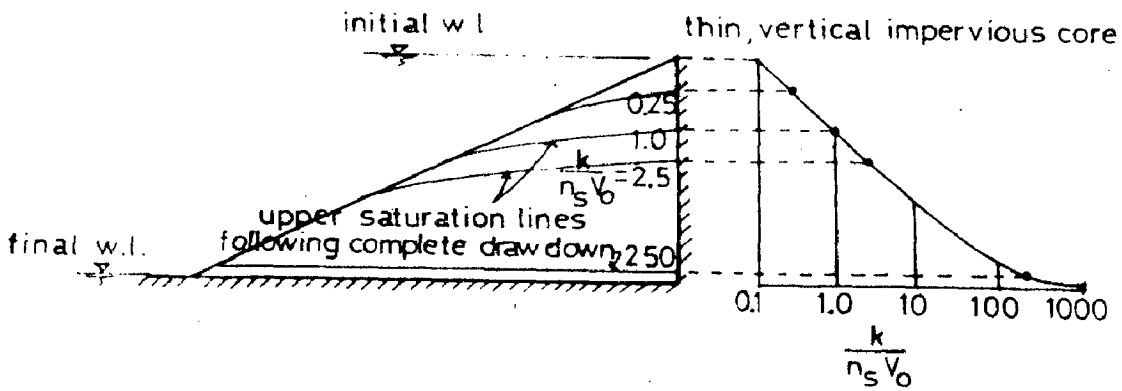


Fig.1.1. Solution by Reinus

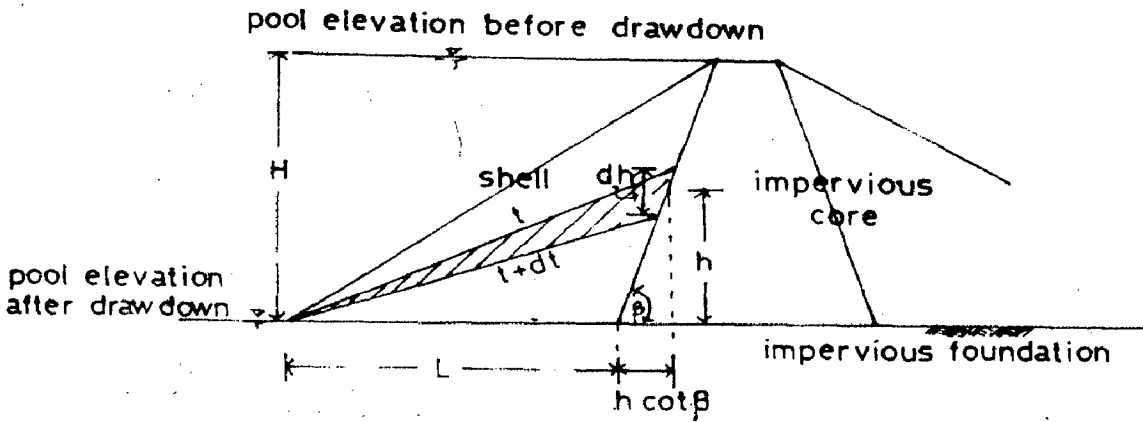


Fig.1.2. A Cassagrande approach

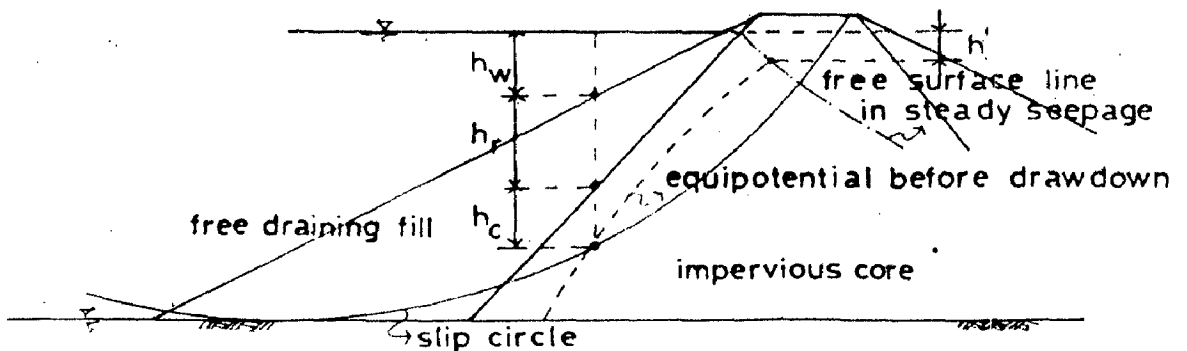


Fig. 1.3. Bishop's approach

h' = potential drop up to the element in steady seepage

n_s = specific porosity of rock fill

For saturated soil $\bar{B} = 1$, and the equation become

$$u = \gamma_w [h_c + h_r (1 - n_s) - h'] \quad (1.25)$$

1.2.3.3 Goel's approach

To estimate draw down pore pressures in an earth dam, Goel (1980) proposed two approaches of mathematical model after taking into account the rate of reservoir lowering and fill characteristic. The first approach is based on Dupuit's assumption and Terzaghi's one-dimensional consolidation theory, whereas second approach is applicable to two-dimensional flow using plane strain approach as applied to Biot's three-dimensional theory of consolidation.

Equation (1.26) and equation (1.27) for first and second approach have been solved using Finite Difference Method (FDM) for known boundary and initial condition.

$$\frac{\partial(h, n)}{\partial t} = K \frac{\partial}{\partial x} \left(h \frac{\partial h}{\partial x} \right) \quad (1.26)$$

where,

h = water head at any time

n = porosity of material

K = permeability of the porous media

$$K_x \cdot \frac{\partial^2 \phi}{\partial x^2} + K_z \frac{\partial^2 \phi}{\partial z^2} = \left[\frac{(1-\mu)(1-2\mu)}{(1-\mu)} \cdot \frac{1}{E_c} + \frac{n}{E_w} \right]$$

$$\gamma_w \frac{\partial \phi}{\partial t} - \frac{(1-\mu)(1-2\mu)}{(1-\mu)} \cdot \frac{1}{E_c} \cdot \frac{\partial \sigma_x}{\partial t}$$

(1.27)

where

- E_c = Young's modulus of soil mass
- μ = Poisson's ratio
- E_w = modulus of elasticity of water
- σ_z = total stress
- γ_w = unit weight of water
- K_x and K_z = permeability in x and z direction respectively.
- t = any time
- ϕ = potential head = $u/r_w + z$
- u = draw down pore pressure
- x, y, z = spatial coordinates of point

1.3 Scope of Problems

In the design process, it is important to estimate the movements, strains and pore pressures which may develop in a dam at various times in its life. Therefore, it is essential to understand the movements and pore pressures which have been measured, the factors which influenced them and the accuracy with which they could have been estimated in advance by theory.

In the case of Rarem Dam, analysis of observed pore pressures will be carried out in various conditions.

To analyze the efficacy of the grouting, an electrical analogy experimental has been carried out in laboratory, because of difference in the permeability of the clay core, grouting zone and foundation zones.

Settlement data is also to be analyzed using Terzaghi's one-dimensional consolidation theory.

2. DESCRIPTION OF RAREM DAM

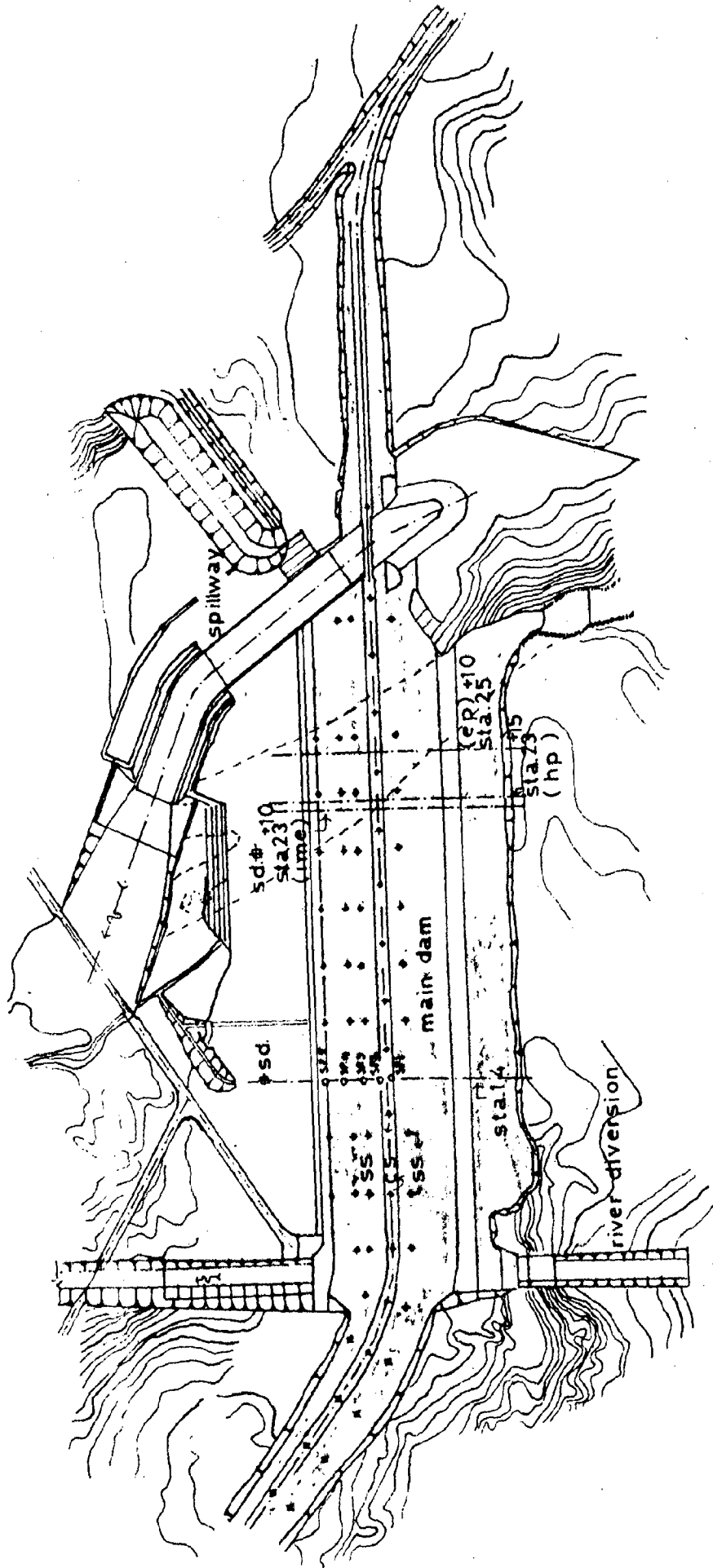
2.1 General Features

The Rarem Dam is located at Pekurun, about 25 km South-West of town Kotabami, North Lampung, Sumatera, Indonesia. The project has created a reservoir with a capacity of 62 Mcum and a ponding area of 1600 HA covering a catchment area of 328 km² which will irrigate an area of 22.000 ha. Rarem dam is zoned type with a clay core flanked by selected sand filter and river run (cobbles and boulders) materials as transition zones respectively. The maximum height of the dam is 28 m and length is 1550 m. The construction of the dam embankment was commenced at the end of November 1981 and completed in the beginning of October 1983. Impounding of the reservoir was performed on the middle of October 1983 i.e. about 2 weeks after completing the dam. The layout of works together with instrumentation plan is shown in Fig.2.1.

2.2 Geology of Dam Site

The project area is widely covered by young sediments of the Andesite Tuff formation which is the product of quarternary volcanic activities and wide-spread in South-Sumatera, composed of tuff-tuff breacias, tuffaceous sandstone and silt stone and andesite.

FIG. 2.1 PLAN OF MEASURING INSTRUMENTS INSTALLATION



- Legend :**
- sp : standpipe piezometer
 - ep : electrical piezometer
 - hp : hydraulic piezometer
 - ime : inclinometer/magnetic extensometer
 - cs : crest measuring point
 - ss : surface measuring point
 - sd : seepage discharge



The dam and reservoir area is located in a hilly region with 30m to 100 m of ground height developed on the foot of the mountainous zone in the south.

The valleys are wide open with mild slope of around 1/10 in gradient on both banks, except for the parts of 10 to 15 m height from the river channel which show occasionally steeper of about 1/2. The river channel forms strong meander incised in residual soil and weathered zone of the bed rock.

Stratigraphic sequence of the dam site geology in order from younger to the older are as follows -

- a) River alluvial deposit, sand and gravels, 5m in thickness
- b) Top soil and residual soil, 5 to 20 m in thickness. Mainly reddish brown clay covering the surface of flat hill on the banks in the level higher than elev + 50 m. A part of this member could be volcanic ash of the most recent time. This material then was used as core zone of the main dam.
- c) The quarternary Andesite tuff formation, more than 60 m in thickness, this forms the foundation bed rock in the dam site.
- d) Diorite, the basement rock, thickness unknown.

The Andesite tuff (bed rock) is a complex of various layers, from less than 1 m upto 10 m in thickness of relatively acidic tuff in various particle size, tuff breccia, conglomerate tuff, tuffaceous sand stone and tuffaceous clay stone.

Weathering infects the zone (5 to 10 m thickness) at the top and so intensive in its upper half portion that the boundary with the overlying top soil and residual soil bed is often obscured.

The river alluvial deposit is well graded mixture of sand and gravel with D_{20} at 20 mm, containing boulders upto 30 cm in diameter. The gravels are largely of andesite and granite origin. It is spread all over the flat bottom of valley with about 5 m of the maximum thickness.

Geological profile along dam is shown in Fig.2.2.

2.3 Dam Section

The Rarem Dam is a zoned type having 28m in height with a vertical central of clay core, the slopes of core is 1V : 0.2 H at the both u/s and d/s. The clay core is protected by selected grade of sand as filter and sand gravel materials as transition zone. The outer u/s slope of 1V:3H and d/s slope of 1V : 2H, of rockfill are adopted based on stability consideration.

A typical cross-section of the dam and its arrangement of instrumentation is shown in Fig.2.3.

The material of the clay core was borrowed from the reservoir area about 2 km from dam site which consists of reddish brown clay, high plasticity, dominated by Kaolinite mineral, would be classified as CH according to the Unified Soil Classification System. While the material of sand as filter and sand gravel as transition zones were taken from the Rarem river deposit. The material for rockfill zone was taken from quarry about 6 km South in a straight line from the dam site which was quarried from the Andesite bed.

2.4 Material Properties

The properties and parameters of soils to be used for the Rarem Dam are as follows -

a) Core Zone (zone 1)

i) Gradation	size (mm)	percent finer
Clay	≤ 0002	29
Silt	0.002 - 0.075	64 - 91
Fine sand	0.075 - 0.500	7 - 9

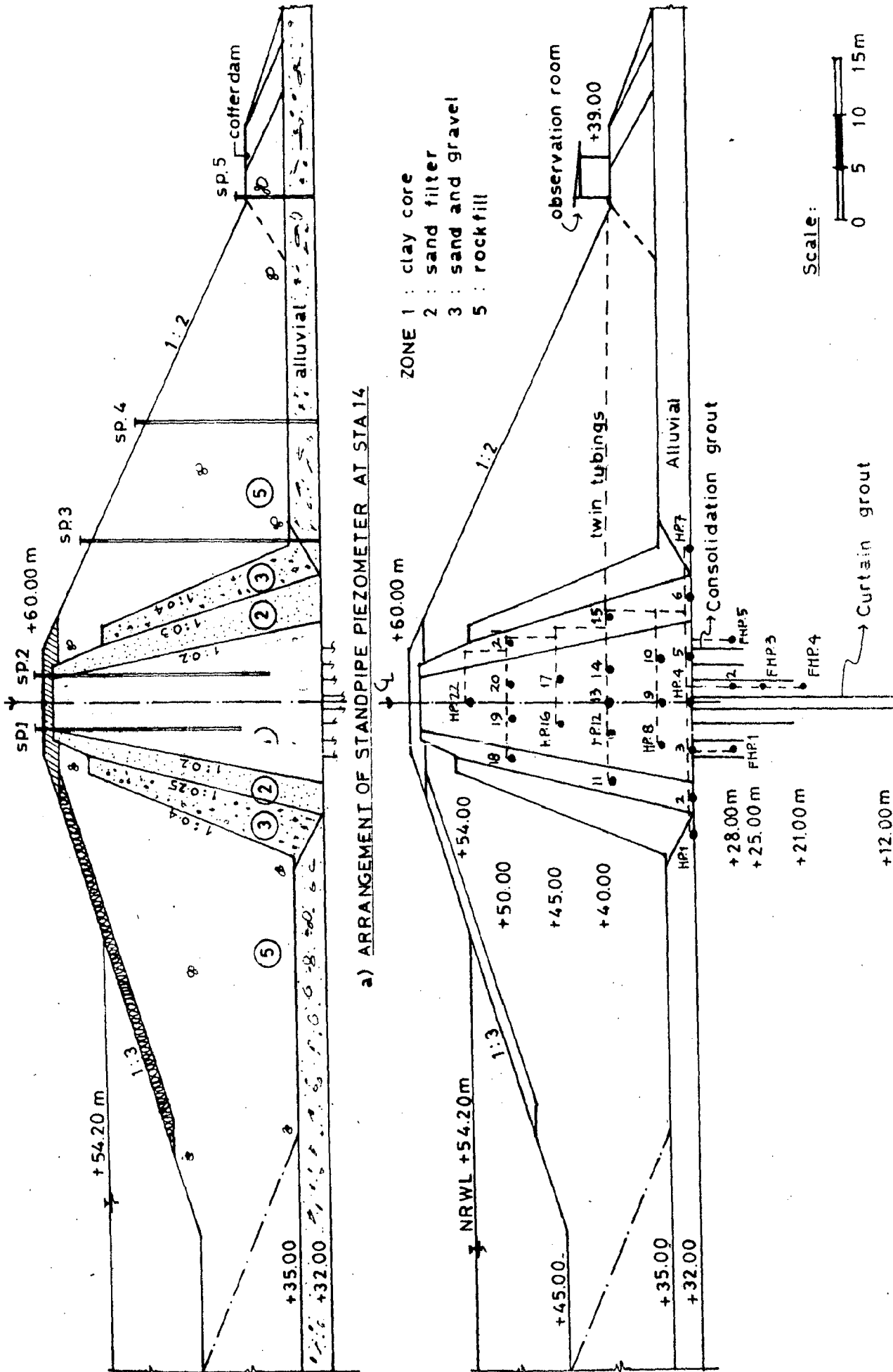


Fig. 2.3^a

- ii) Atterberg limit (average values)
 - liquid limit, LL = 96.4 percent
 - plastic limit, PL = 48 percent
 - plasticity index, PI = 48.4 percent

iii) Laboratory compaction test (average)

$$\gamma_{d \text{ max}} \text{ (t/m}^3\text{)} = 1.10 - 1.12$$

$$\text{OMC (percent)} = 48.80 - 50.50$$

iv) Specific gravity, SG = 2.68

v) Shear strength - $C \text{ (t/m}^2\text{)} = 1.0$

$$\phi \text{ (degree)} = 28$$

vi) Permeability (cm/sec) = 5.9×10^{-6}

b) Filter Zone (zone 2)

i) Gradation	Size (mm)	Percent - finer
Fine sand	0.075-0.450	20 - 40
Medium sand	0.450 - 2.000	50 - 48
Coarse sand	2.00 - 4.500	12 - 14

ii) Shear strength - $C \text{ (t/m}^2\text{)} = 0$

$$\phi \text{ (degree)} = 36$$

iii) Unit weight, $\gamma_n \text{ (t/m}^3\text{)} = 1.987$

Moisture content, w(percent) = 9.64

Void ratio, e = 0.411

Saturation, S(percent) = 80

Specific gravity, SG = 2.55

iv) Permeability, $K(\text{cm/sec}) = 1 \times 10^{-3}$

c) Transition Zone (zone 3)

i) Gradation	size (mm)	Percent - finer
Sand	≥ 4.5	18 - 28
Gravel	45 - 75.0	67 - 62
Cobbles	75.0-150.0	38

ii) Unit weight, $\gamma_n(\text{t/m}^3) = 2.192$

Moisture content, $w(\text{percent}) = 7.25$

Void ratio, $e = 0.286$

Specific gravity, $SG = 2.63$

iii) Shear strength, $C(\text{t/m}^2) = 0$

$\phi(\text{degree}) = 38$

d) Rockfill Zone (zone 5)

i) Gradation 0.30 - 350.0 mm

ii) Unit weight, $\gamma_n(\text{t/m}^3) = 2.0$

Saturated unit wt, $\gamma_{\text{sat}} = 2.2$

Specific Gravity, $SG = 2.52$

iii) Shear strength, $C(\text{t/m}^2) = 0$

$\phi(\text{degree}) = 40$

2.5 Foundation Treatment

Foundation treatment was carried out solely by means of grouting for foundation of the main dam, the river diversion conduit, the spillway weir and the intake structure. The works comprises of the following -

a) Curtain grouting which was performed in the dam axis with grout holes arranged on two lines, one meter apart from each other at staggered position. Spacing of the holes on each line was 1.5 m with the depth ranging from 5 m to 20 m.

b) Consolidation and blanket grouting
These groutings were performed in the u/s and d/s sides of the curtain grouting at the bottom of the cut-off trench for the section between Sta 1 and Sta 28. The grout holes were arranged at 3m interval on six parallel lines, 1.5 m apart from each other. The holes were drilled up to 10 m deep on the lines adjacent to the curtain grouting and 5 m on the other lines.

The consolidation and blanket groutings were done prior to performing the curtain grouting.

2.6 Instrumentation

2.6.1 Necessity

The main purpose of instrumentation in a dam is to monitor the continued safety of the structure, as well as

to provide a check on the design assumption and method of computation in vogue.

Instrumentation would be effective and worthwhile only if it provides sufficient reliable data from which the safety and performance of the embankment can be reasonably and reliably evaluated.

The requirement of an effective instrumentation are that the measuring devices should be simple in design, must be robust and reliable, minimum maintenance, requiring minimum skilled man power, minimum overall cost and the data obtained should be meaningful which it can be easily interpreted.

The following types of instruments have been installed at the Rarem Dam.

- a) Electrical Carlson type piezometers for measuring pore water pressures.
- b) Hydraulic piezometers for measuring pore pressures
- c) Standpipe piezometers for determining the phreatic line.
- d) Internal instruments (Inclinometer/magnetic extensometer) for measuring horizontal movements and vertical displacement (settlement).

- e) Surface monuments for measuring horizontal and vertical deformation at the surface.

2.6.2 Piezometers

In most dams a main battery of piezometers is set into one or more transverse sections of the dam to give a general information of the pore pressure distribution. Additional piezometers are then placed at spot where specific information needed. Three basic types of piezometers have been installed in the Rarem Dam -

The piezometer tips have been embedded both in embankment fill and foundation of the dam. Foundation model piezometers were installed in drilled holes, while embankment models, though some times also located in drilled holes, were placed in the fill as it was being constructed.

Three basic types of piezometers have been installed in the Rarem Dam -

- a) Electrical Carlson type piezometers, installed at Sta. 25⁺¹⁰ - total 27 nos.
- b) Hydraulic Bishop type piezometers, embedded at Sta. 23⁺¹⁵ - total 27 nos.
- c) Stand pipe (Cassagrande porous tip) piezometers, installed at Sta. 14 - total 5 nos.

Out of 27 nos electrical types piezometers, 7 nos were found damaged during calibration stage and ~~out~~ remaining of 20 nos, 14 nos. also became out of order during construction period.

R. Post and J. Picaut (Coyne et Bollier, Paris - Proceeding of the 7th International Conf. on SMFE, Mexico, 1969, Vol.3, p. 431) have compared the performance of these electrical and hydraulic types -

- i) Pressures as measured by electrical cells usually differ by one to two metres of water exceptionally up to 5 m.
- ii) The proportion of instruments out of order after 12 years of measurement at one dam, is very small for both types, being 5 percent on average, for a total of 121 electric cells and 80 hydraulic cells, damage occurred on installation or shortly afterwards.
- iii) The use of porous stone with high air entry values for both types of cells as compared to the use of coarse stones did not affect the measurement of pore pressures in the core during construction. The use of high air entry stones reduces scattering of the readings of the hydraulic cells and permits the measurement of negative pore pressures

with the electrical cells only during a limited time after placement, because of air diffusion through the stones.

- iv) Both installation and measurement appear to be easier and more rapid with electrical cells. Moreover, these can be placed at any level in relation to the reading station.
- v) Cost, including installation is in the same range for both types.

While A.W. Bishop (Proceeding of the 7th International Conference on SMFE, Mexico, 1969, P. 429) described the advantages and disadvantages of hydraulic piezometers as follows -

Advantages -

- i) Continuity with the pore water can be re-established in partly saturated soils
- ii) Pressure measurement is external, calibrations can be checked and there are no moving parts to give trouble in long term operation.
- iii) The operation of the piezometers can be checked in situ.
- iv) The piezometer, can often be used for measuring in-situ permeability.

Disadvantages -

- i) Cavitation within the connecting tubes restricts the relative elevation of the piezometer tip and the measuring point.
- ii) De-airing and pressure measuring devices may require large instrument houses
- iii) De-airing may be required, every few weeks if suction are being measured and at interval of several years at positive pressures.
- iv) Hydraulic systems are subject to freezing in cold climate.
- v) Blockages may occurs if clean water is not used.

Again as reported by Coaling (1962) that the electrical transducer is not always reliable under field conditions, especially under long term use, because it is impossible to recalibrate once the piezometer is in the ground.

While Hosking and Hilton (1963) reported that the leads from their vibrating wire piezometers to the reading station were the weakest link in the system.

In the case of the Rarem Dam, as mentioned earlier, the electrical Carlson type piezometers mostly were found out of order being calibrated or installation period.

The causes of damaged piezometers were suspected as under -

- i) The wire gauges were broken due to vibratory or sudden shocking or hitting being transported from their manufacture to the site.
- ii) After embedding piezometer tips in the foundation or fill for a few periods, the seal was leaking and water entered into the cells causing short circuiting in the system.

Prior to installation, each set of piezometer tip was tested and soaked into the water until saturated and carried down carefully into a drilled hole on the dam foundation. Selected filler sand is then placed around it and a cement bentonite sealing is placed above it.

The embankment model piezometers are installed during earth fill placement when the fill has reached the required elevation. A trench about 0.70 m deep is dug from the position of the bore hole to the observation room. The lines of piezometers are placed in this trench.

The tips are carefully saturated with de-aired water and taken on site under water. The connecting tubes, which have been carefully de-aired from the observation room by flushing with de-aired water are connected to the tip under water.

The tip is then lifted out of the water and carefully pressed into the special hole digged for it Readings are taken and several checks are made during trench backfilling and during placement of about 1 m of fill for accidental damage to the tip. To prevent the seepage which may pass through between soil and its tubes, a soil-bentonite mixture. Seal is provided at several intervals.

Standpipe piezometers were installed at Sta.14 by means of drilling holes. SP1 and SP2 at the crest in the core zone, SP3 and SP4 on the downstream slope of rock zone and SP5 on the crest of the downstream Cofferdam. Type of the piezometer tip is Cassagrande porous plastic protected by perforated rigid pvc pipe. The top of each pipe is protected by concrete box and a lockable steel cover.

2.6.3 Inclinator/magnetic extensometer

One set of uniaxial inclinometer/extensometer was installed at Sta 23⁺¹⁰ vertically on the center line of core zone. The instrument consist of access tubes of alluminium with grooves in four directions perpendicular each other, magnetic settlement plates surrounding the access tube, a specific torpedo with an electrical cable and a digital read out unit.

By lowering the probe into the access tube it can show the inclination of the access tube on the read out digital. The position of magnetic plates can be detected by using a reed switch probe which is lowering into the access tube.

The access tube was embedded into a drilling hole which was prepared for it.

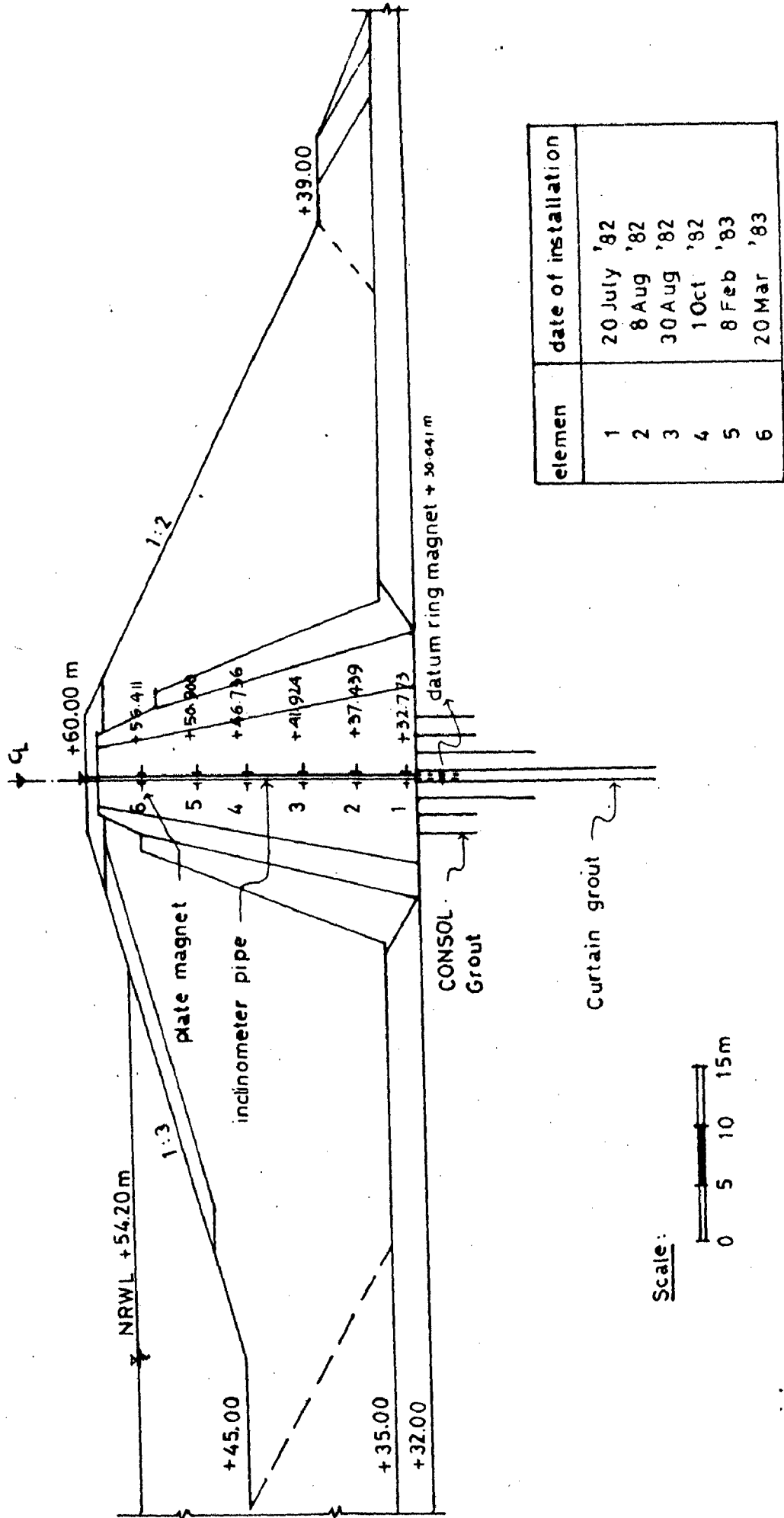
The arrangement and initial elevation of the magnetic plates can be found in Fig.2.3b.

2.6.4 Surface Monuments

Thirty seven points of the surface monuments have been placed at the crest and 61 points on the slopes of dam for monitoring the displacement at the surface of the dam body. Twenty four out of 61 points were burried on u/s slope and the remaining on the d/s slope. Bench Marks and targets for cordinating survey were provided on concrete abutment of the spillway for periodical measurement.

The crest measuring points consisting of 100 mm diameter galvanized steel pipe, 2 m in length were embedded into the completed core zone which excavated by a back hoe and refilled by hand operated tamper, the upper part of this device was covered by a concrete block.

Fig. 23^b ARRANGEMENT OF INCLINOMETER/EXTENSOMETER AT STA 23⁺¹⁰



Otherwise, the slope surface measuring points consisting of 150 mm diameter galvanized steel pipe 2 m in length, were installed into the outer surface of the completed rock zone. These points are located in rows at approximately 40 m spacing on lines parallel to the centre line of the dam at elevation + 55.00 u/s and at ele. + 53.00 m and + 39.00 m d/s slope.

2.7 Quality Control and Monitoring

2.7.1 Quality Control

The quality control on the dam embankment was done under the full responsibility by the Engineer. The manual on Quality Control of dam embankment was delivered to the contractor prior to the commence of the works. The manual shows every detail of engineering tests in-situ and indoor required. Site soil-concrete laboratory was established for testing the engineering properties of materials and supplied with the adequate testing apparatus.

Engineering tests applied for quality control of embankment were conformed to the ASTM and JIS.

The equipment used for compacting each zone are as follows -

Zone	Spreading thickness (cm)	Equipment used	Roller passes
Zone 1 (clay core)	25	Tamping roller	8
Zone 2 (sand filter)	25	Vibratory roller	8
Zone 3 (transition)	70	Bulldozer (D-8)	4
Zone 5 (rockfill)	100	Bulldozer (D-8)	4

The result of the routine tests for zone 1 as evaluated by statistical approach are summarized below -

Sl. No.	Lab. compaction test		Field test			
	Avg. of OMC (percent)	Avg. of MDD (t/m^3)	Placement (percent)		Field density, MDD (percent)	
			Avg.	Standard deviation	Average	Standard deviation
1	48.30-50.50	1.10-1.12	50.30	1.34	101.8	1.94

For zone 2 (sand filter), Lab. compaction test was performed by means of relative density test which the average minimum value was $1.459 t/m^3$ and maximum value of $1.968 t/m^3$, since the average of in-situ density test was $1.836 t/m^3$ at moisture content of 9.64 percent. The laboratory relative density test resulted a minimum value of $1.54 t/m^3$ and

maximum value of 2.15 t/m^3 , while the average dry density obtained from the field test resulted 2.045 t/m^3 at moisture content of 7.25 percent for zone 3 (transition zone).

Other laboratory tests on material of zone 1 were also carried out such as permeability test, triaxial and consolidation test for comparing and checking from design parameter values.

2.7.2 Monitoring

The frequency of periodical observation on instruments was recommended to the project as follows -

Sl. No.	Measuring devices	Frequency of period		
		Loading test	Stabilization	Maintenance
1.	Piezometers	twice a week	Once a week	Once a month
2.	Inclinometer/ extensometer	once a week	once a month	twice a yr.
3.	Surface monuments	twice a month	once a month	-do-

Note - 1) Loading test means one month prior to impounding to one year after filling the reservoir.

2) Stabilization period follows up to four years after filling

3) Maintenance is the period after stabilization.

3. PRESENTATION AND ANALYSIS OF OBSERVATIONAL DATA

3.1 PORE PRESSURES

3.1.1 Presentation of Observational Data

3.1.1.1 Hydraulic piezometer data

The construction of the dam embankment was begun at the end of November 1981, whereas the installation of foundation type piezometer was started in July 1982 after completion of grouting works and pore pressure observations were started from August 1982 when the fill reached elevation + 37.00 m. The reading was continued according to the recommended procedure of monitoring until December 1985, except a gap of reading from January to December 1983. The dam was completed in October 1983 and the reservoir filling started immediately thereafter. The reservoir was filled by mid of January 1984.

Five foundation tips have been installed in the tuff rock-foundation of dam, FHP 1, FHP 2 and FHP 5 embedded at elevation 28.00 m, FHP 3 and FGP 4 at elevation 25.00 m and + 21.00 m respectively. The observed pore pressures in these foundation piezometer tips are shown in Fig.3.1.a.

A total of 22 nos. embankment type hydraulic piezometers have also been embedded in the body of dam as shown in Fig.2.3a. A study of this figure indicates that the piezometers are installed in 6 tiers, viz. seven piezometers HP.1 to HP.7 in first tier (El.+ 32.00 m), three piezometers

HP 8 to HP.10 in second tier (El.+ 35.00 m), five piezometers HP.11 to HP.15 in third tier (El + 40.00 m), two piezometers HP.16 to HP.17 in fourth tier (El.+ 45.00 m), four piezometers HP.18 to HP.21 in fifth tier (El.+ 50.00 m) and one piezometer HP.22 in sixth tier (El.+ 54.00 m). Piezometers HP.1 and HP.7 were installed in alluvium and piezometers no.HP.11, HP.15, HP.18 and HP.21 were installed in sand filters, other remaining piezometers were installed in clay core. Pore pressure observation for tips no.HP.1 to HP.11 are shown in Fig.3.1.b, HP.8 to HP.15 in Fig.3.1.c and HP.16 to HP.22 in Fig.3.1d.

3.1.1.2 Electrical Carlson type piezometers

As described earlier, 27 nos. electrical type have been installed at sta. 25⁺¹⁰. Despite very careful checking and calibrating of this type, a lot of them were found out of order. Out of 27 nos., only 6 nos. were working, but their readings showed erratic and unreliable values. Nevertheless hydraulic piezometers are functioning very well and are giving reliable information, so that data of electrical Carlson type piezometer is not presented herein.

3.1.1.3 Stand pipe piezometers

Five Cassagrande type piezometers (SP.1 to SP.5) were installed at St.14, about 180 m far from Sta.23⁺¹⁵ (hydraulic piezometers). The reading of water levels in the stand pipes were taken soon after the installation completed

in January 1984. SP.1 and SP.2 were installed in clay core, SP.3 to SP.5 in downstream shell comprising rock zone. The observational pore pressure data is presented in Fig.3.1.e.

3.1.2 Analysis of Pore Pressures Data

3.1.2.1 Pore pressures in foundation

A study of Fig.3.1.a showing pore pressures of foundation tips FHP.1 to FHP.5 indicates that during construction period (April to December 1982), the pore pressures recorded vary from El.+ 31.00 m to El.+ 33.00 m meaning thereby that during this period the pore pressures correspond to river bed level of El.+ 32.00 m. During reservoir filling period, October to December 1983, these tips have recorded increase in pore pressures following the pattern of reservoir level raising almost simultaneously. Since the reservoir level has remained almost constant from January 1984 onward, the pore pressures recorded by the five foundation piezometers are also almost constant. Variation of the order of + 1.0 m water head may be due to inherent humitation of the instrumentation. Observations during and after reservoir filling indicates that for FHP.1, FHP.2 and FHP.5 located at El.+ 27.00 m, their pore pressures reduce from tip no.FHP.1 to FHP.3 indicating thereby the effect of consolidation grouting done upto El.+ 27.00 m. Tip no.FHP.4 (El.+21.00 m) located at the lowest level and downstream of grout curtain has recorded the highest pore pressure, similarly FHP.3 located downstream of grout curtain at El.+25.00 m has also shown higher pore pressure

than that recorded by FHP.2. Recording of higher pore pressures by FHP.3 and FHP.4 as compared to FHP.2 is contrary to well established theories with a view to try to explain this anomaly. , an electrical analogy experiment was carried out, the details of which are given in Chapter 4.

According to Cassagrande (1961), the effectiveness or the efficiency of the grout curtain has been defined as the ratio of $(q_1 - q_c) / q_1$ - where :

q = Seepage through the foundation without grout curtain

q_c = similar but with grout curtain

In the absence of any data with regard to the seepage quantity, the efficiency of the grout curtain was determined from the decrease in pressure heads using the formula (Hari Krishna and Goel, 1978) :

$$\text{Efficiency} = (p_1 - p_2) / p \times 100 \text{ percent} \quad \dots (3.1)$$

where :

p_1 and p_2 = the pressure heads upstream and downstream of the grout curtain respectively

p = effective reservoir head. The efficiency

of the grout curtain has been calculated by taking total head corresponding to observed piezometer head in tip no. FHP.1 and tail water level as recorded in a stand pipe piezometer embedded at toe of dam at sta.14 about 180 m far from Sta.23⁺¹⁵. The recorded tail water level is at

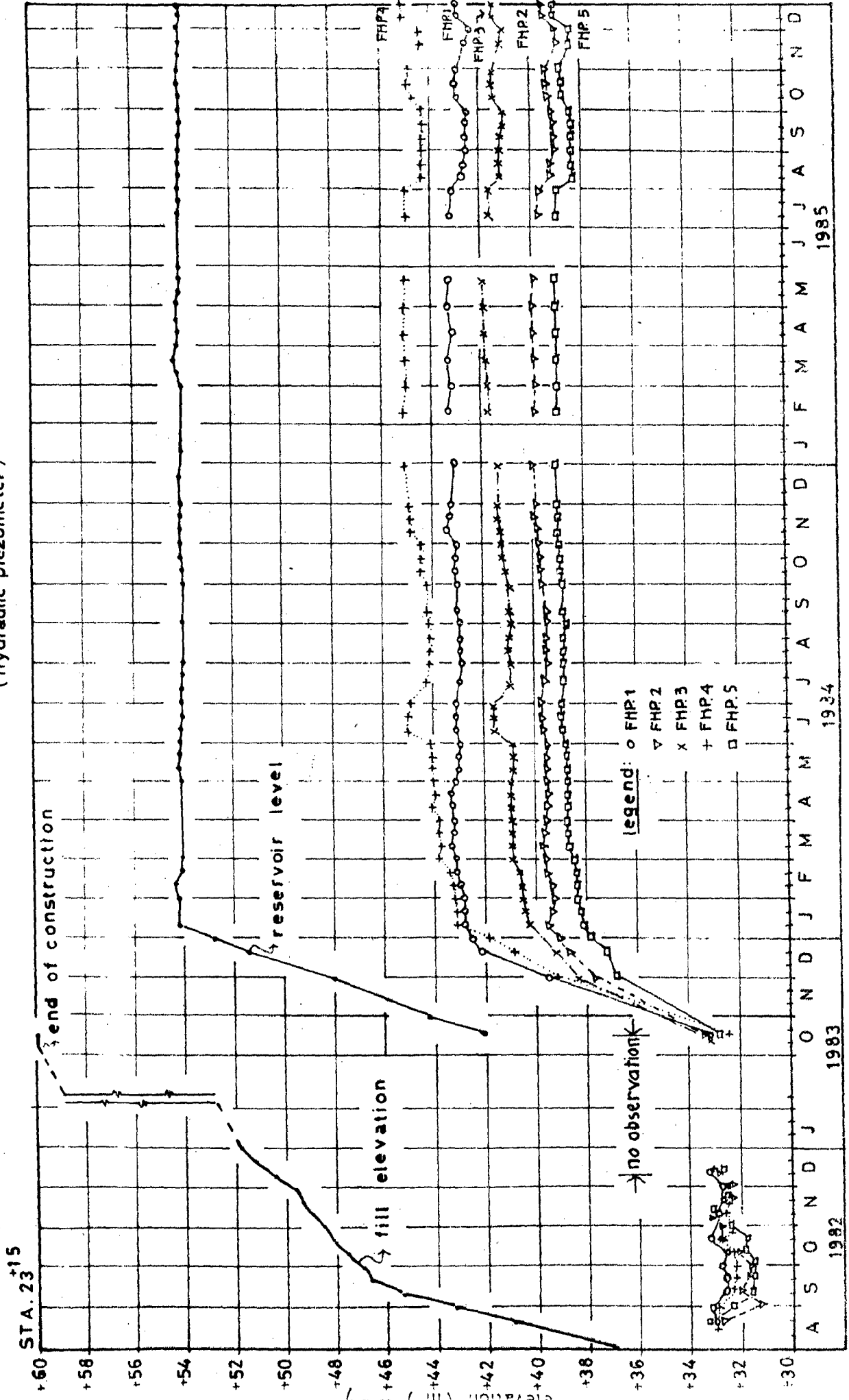
El.+32.50 m whereas recorded elevation of pore pressure in FHP.1 is + 43.30 m. The results of calculation of grout curtain efficiency based on this approach are shown in Table No.3.1.

Table 3.1: Grout Curtain Efficiency Based on Observed Pore Pressure

Sl. No.	Elevation (m)	Piez. No.	Observed pore pressure (m)	$p_1 - p_i$ at the same El.+28.00m	Eff. = $(p_1 - p_i) / p \times 100$ percent
1		FHP.1	$p_1 = 15.3$	0	0
2.	+28.00	FHP.2	$p_2 = 11.5$	3.8	35.19
3.		FHP.5	$p_5 = 10.5$	4.8	44.45
4.	+25.00	FHP.3	$p_3 = 15.7$	2.6	24.07
5.	+21.00	FHP.4	$p_4 = 23.2$	-0.9	-8.33(not accepted)

Cedergren (1948) offered a solution in determining the efficiency of the grout by drawing a flow net and taking the permeabilities of foundation and grouting zone into account. In the case of Rarem Dam, not only grout curtain is there, but consolidation grouting is also provided, so that the problem would be complex, if it had been solved by graphical method. An electrical analogy experiment to simulate the anisotropy in permeability is suggested to be adopted.

Fig. 3.1.^a PORE PRESSURE OBSERVATION
(hydraulic piezometer)



3.1.2.2 End of construction pore pressures

(a) Observed pore pressures :

Fig.3.1.b depicting pore pressures of HP.1 and HP.2 at El. + 32.00 m reveals that during construction (April to December 1982), the values measured by both piezometers are very close, almost constant of the order of 2 to 2.5 m of water head approximately. It is clear, since the two piezometers were embedded in alluvium or filter zone having high permeability and their values are not affected by the increase in fill height and hence no excessive pore pressures are developed. The value of 2.5 m water head corresponds to the ponding water level at upstream, where the water level of the river is also at El.+ 34.00 m approximately.

Pore pressures recorded by HP.6 and HP.7 buried downstream of core in filter zone and alluvium respectively are of the order of 0 to 1 m (El.+ 33.00 m) and thus are lesser than those recorded by tips located upstream of clay core in similar type of strata.

Pore pressures measured by HP.3 and HP.4 embedded in the clay core show that their values tend to follow the increasing trend as height of embankment fill increases. Their values vary from El. + 35.00 m to + 37.00 m, i.e. pore pressure head of 3 to 5 m water head is recorded. At 5 m pore pressure head, corresponding dam height is 19 m (El.+ 51.00 m = El.+32.00 m). This means that for the

clay core belonging to CH-group, placed at 1.5 percent dry of OMC, construction pore pressures developed are of the order of 25 percent. Nevertheless the reading of HP.5 which is also embedded in the core, indicates that its pore pressure value is almost constant and is of low order (1 to 2 m). This may be due to the fact that the tip might have been installed in the foundation material rather than in clay core material, because this tier of tips is at the junction of clay core and foundation material.

A study of Fig.3.1.c and 3.1.d indicates that no significant pore pressures development was recorded by HP.8, HP.9, HP.10, HP.12, HP.13, HP.14, HP.16 and HP.17 embedded in the core zone during construction period of their location and zone of embankment. Not only this but also some negative pore pressures were recorded by tips no.HP.19, HP.20 and HP.22 respectively. The negative values of HP.11, HP.15, HP.18 and HP.21 are clear, because they are located in the filter zone.

The core material consists of high plasticity reddish clay, classified as CH - group having PI about 48 percent and coefficient of permeability about 6×10^{-6} cm/sec., indicates that the clay material is compressible enough and excess pore pressures during construction should have been developed. However, the pore pressures recorded during brief period of observation (August - December 1982) does not confirm this. More positive conclusion

would have been possible at the observations continued beyond December 1982 till March 1983, the period during which the dam height was raised further by 8 m. Development of low construction pore pressures may be due to fill placement on dry side of OMC (- 1.5 percent), low placement densities (dry density = 1.12 t/m^3) and possibility of arching action.

(b) Hilf's pore pressure

An estimation of pore of pore pressures at the end of construction was done based on the Hilf's method with no dissipation factor involved into account using consolidation test data. The results of this study are shown in Table 3.2.

$$\gamma_d = 1.12 \text{ t/m}^3 \text{ and } \gamma_n = 1.65 \text{ t/m}^3$$

$$w = 47.06 \text{ percent}$$

$$G = 2.68$$

$$n_o = 58.20 \text{ percent}$$

Henry's constant being equal to 0.0198.

Volume of water in voids,

$$\begin{aligned} V_w &= w \cdot \gamma_d = 47.06 \times 1.12 \\ &= 52.71 \text{ percent} \end{aligned}$$

Initial degree of saturation,

$$S_o = \frac{V_w}{n_o} = \frac{52.70}{58.20} = 0.906$$

Fig.3.1. ^b PORE PRESSURE OBSERVATION
(hydraulic piezometer)

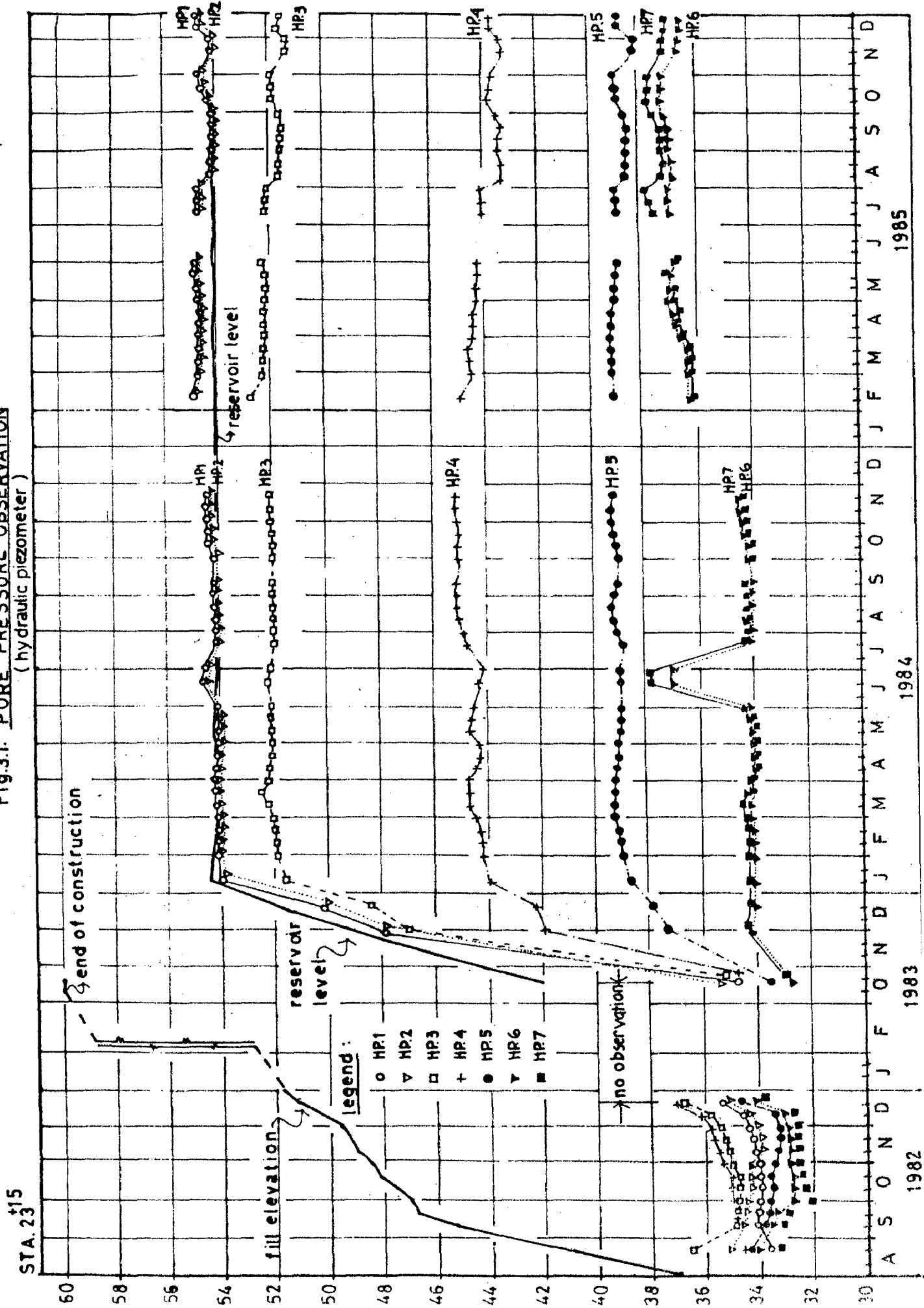


Fig. 3.1^c PORE PRESSURE OBSERVATION
(hydraulic piezometer)

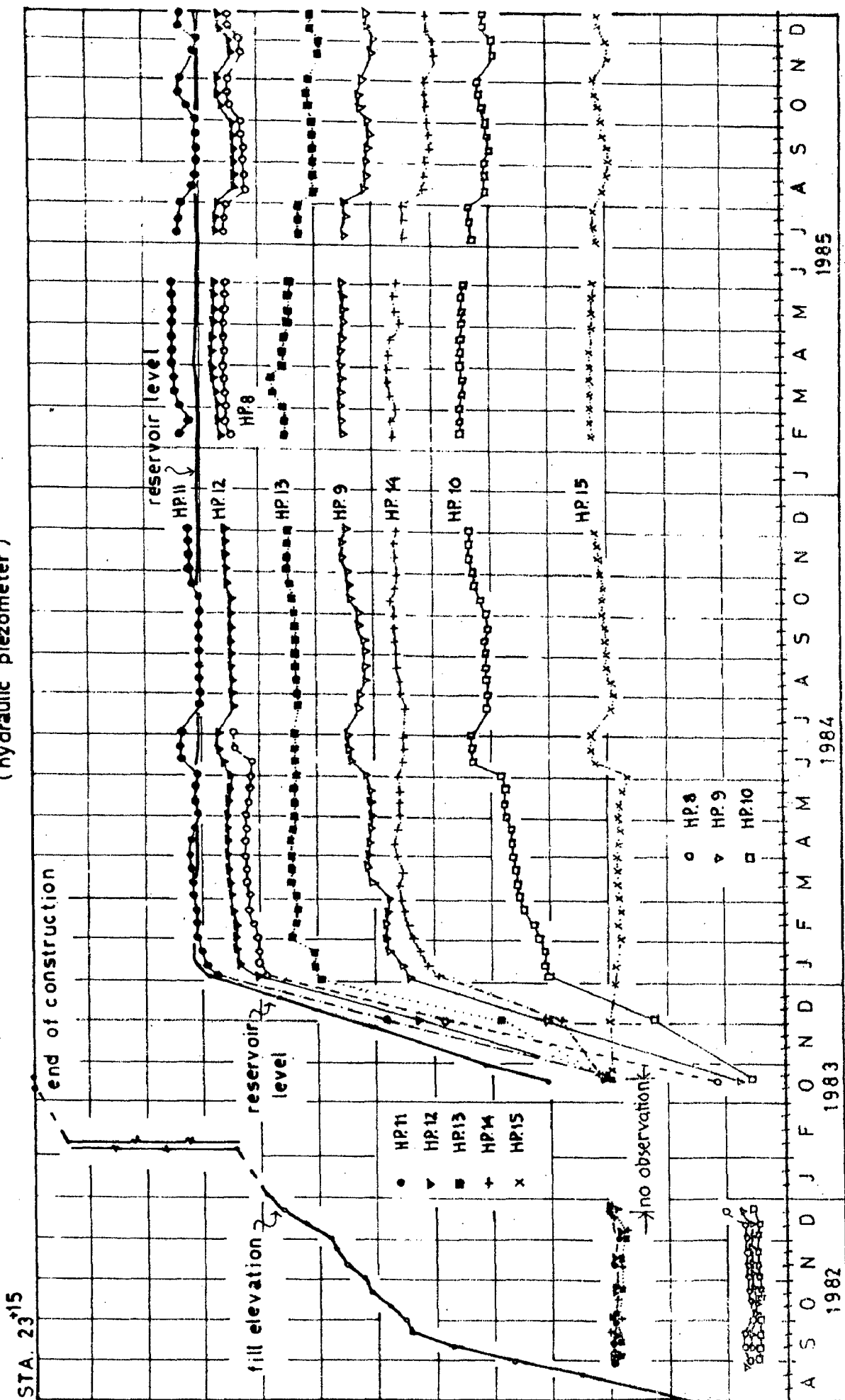


FIG. 3.1. PORE PRESSURE AND SETTLEMENT OBSERVATIONS

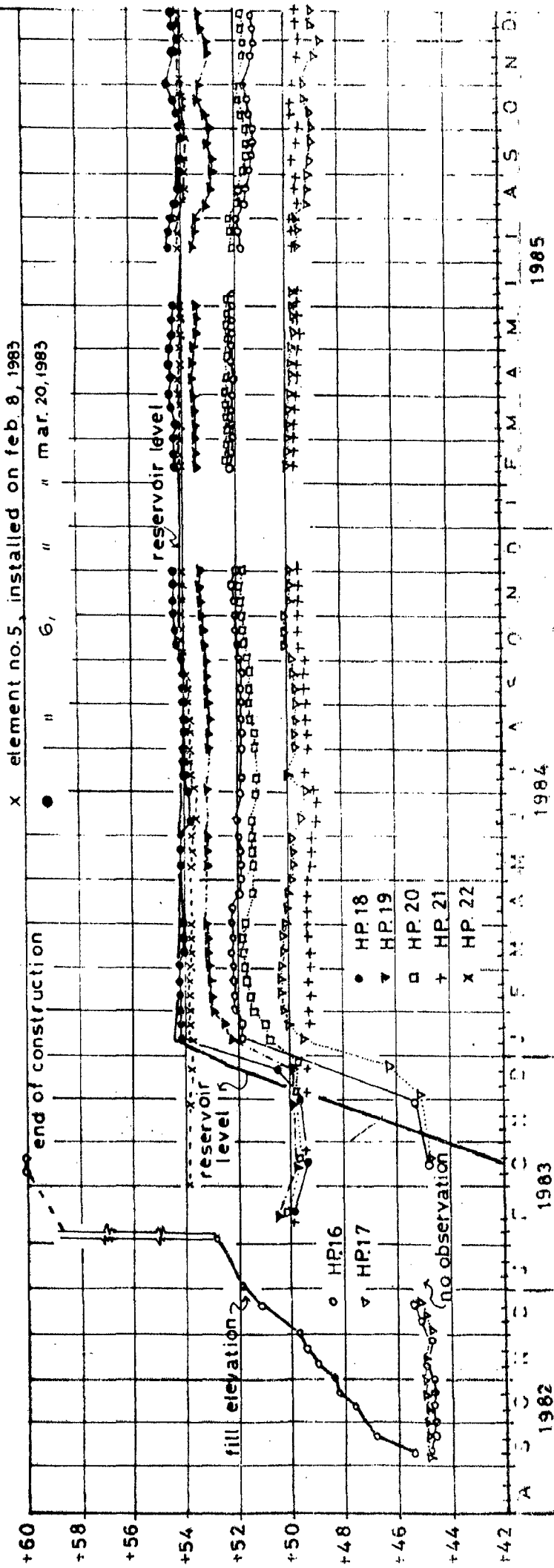
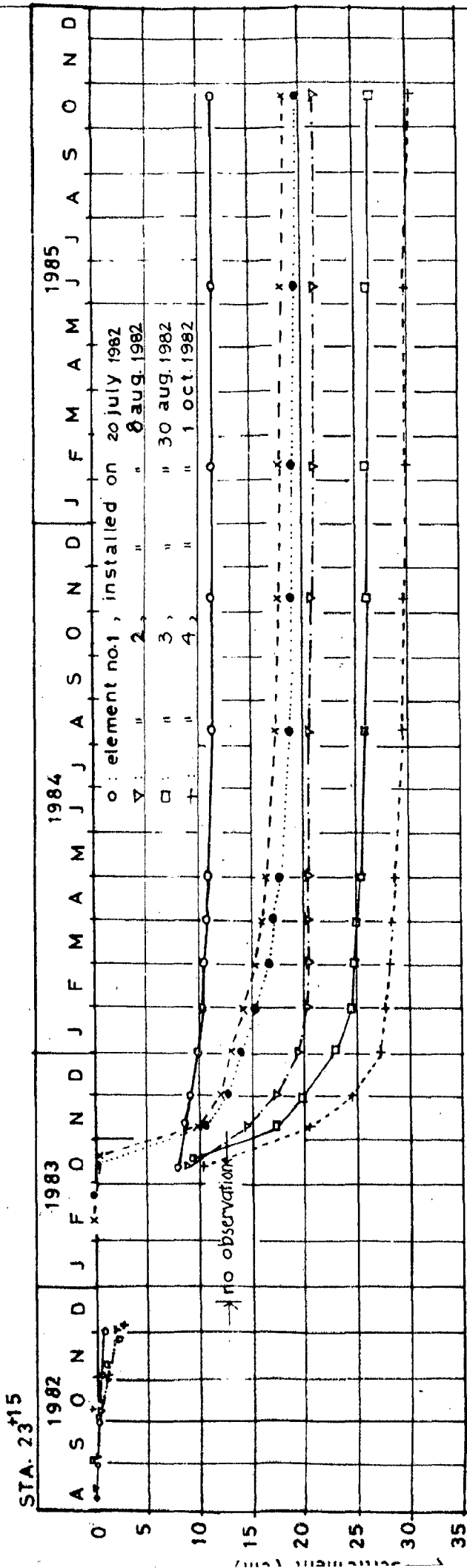
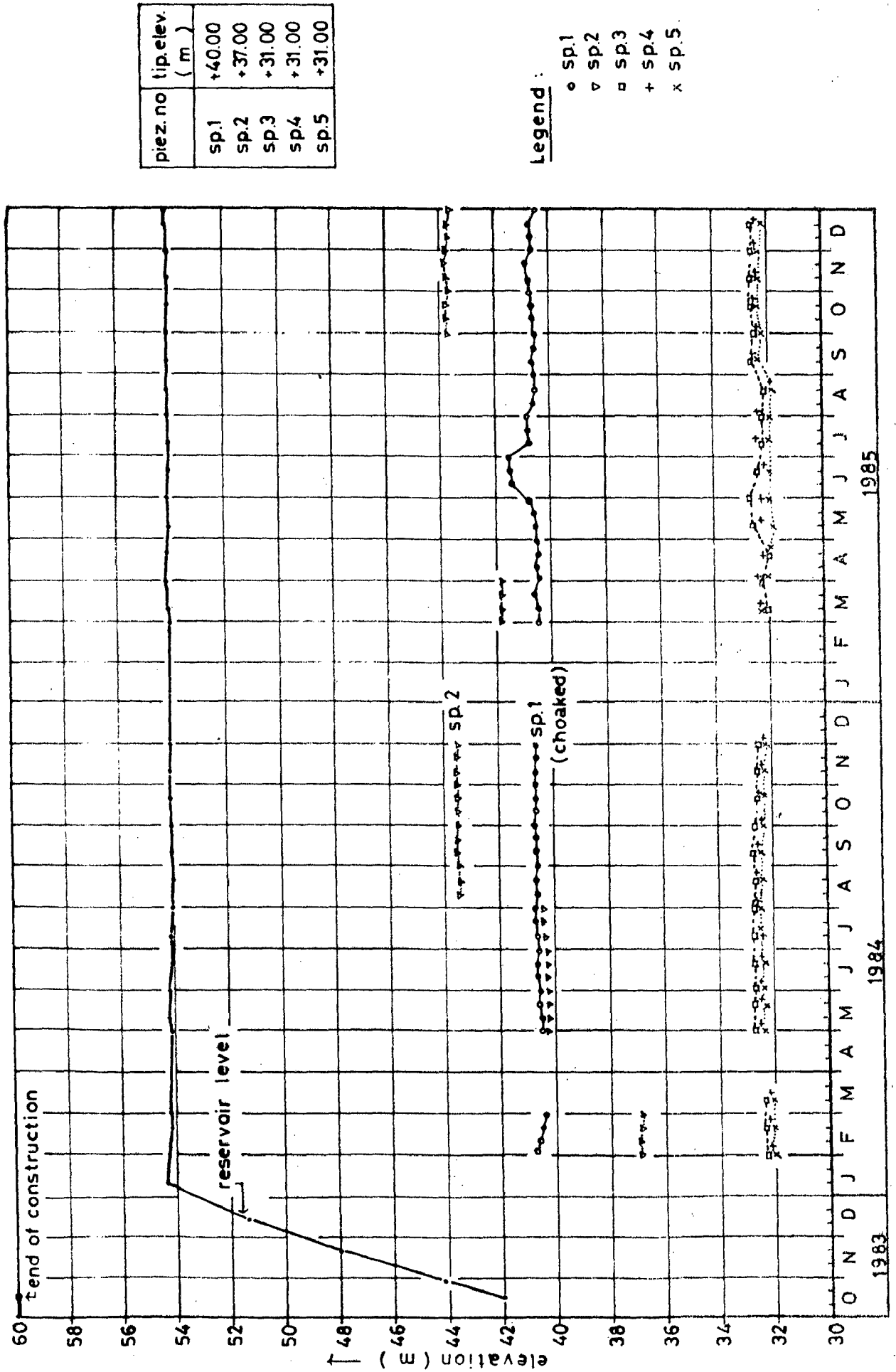


Fig. 3.1^o STANDPIPE PIEZOMETER - WATER LEVEL OBSERVATION

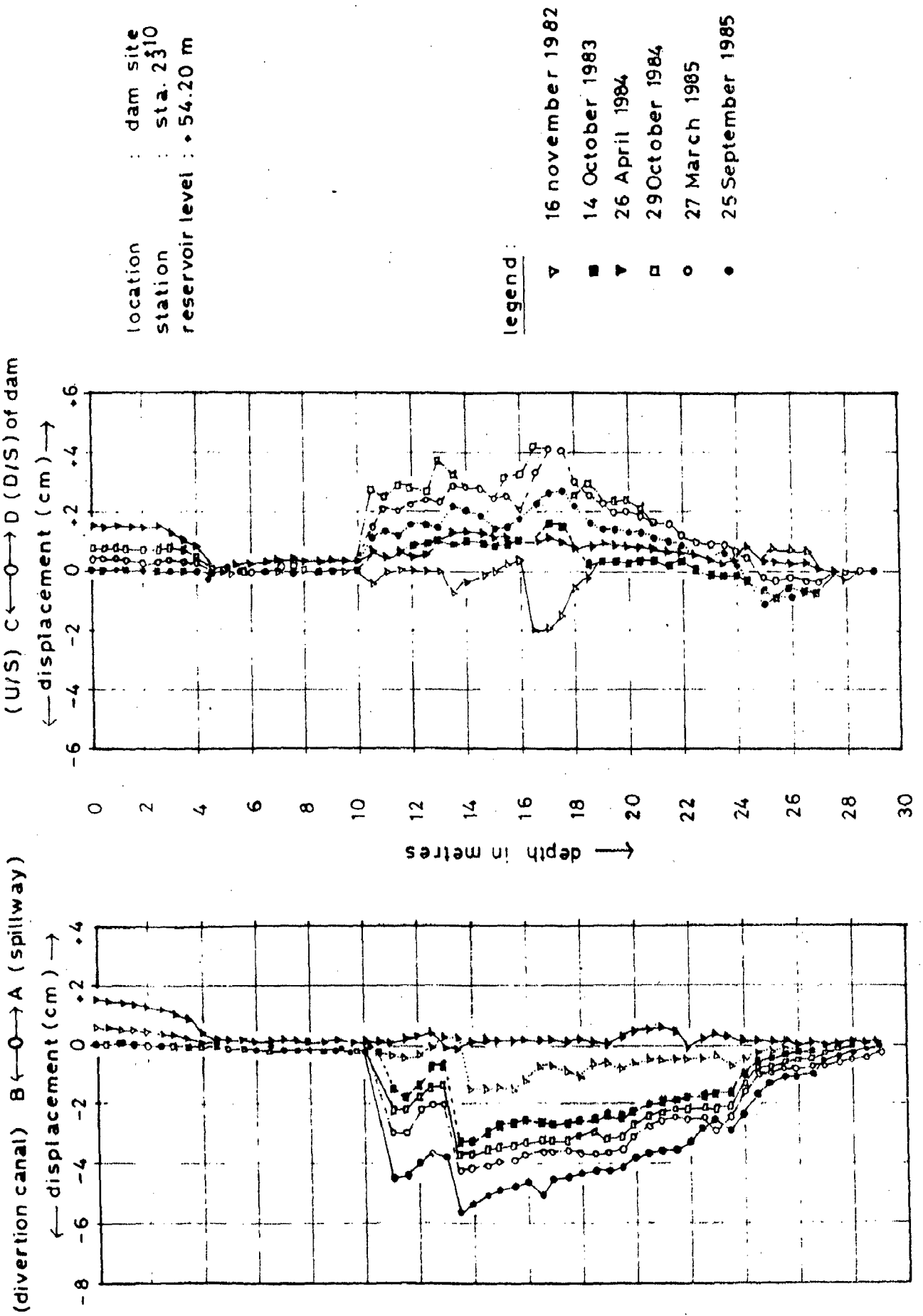


piez. no	tip elev. (m)
sp.1	+40.00
sp.2	+37.00
sp.3	+31.00
sp.4	+31.00
sp.5	+31.00

Legend :

- o sp.1
- ▽ sp.2
- sp.3
- + sp.4
- x sp.5

Fig.3.1 GRAPH OF INCLINOMETER READING



Volume of dissolved air,

$$HV_w = 0.098 \times 52.71 = 1.044$$

Volume of free air,

$$V_a = n_o - V_w = 58.20 - 52.71$$

$$= 5.49 \text{ percent}$$

Total volume of air at atmospheric pressure,

$$p_o = V_a + HV_w = 5.49 + 1.044 = 6.534 \text{ percent}$$

Table 3.2 : Hilf's Construction Pore Pressures for Clay Core Using Consolidation Test Data

Sl. No.	Effective stress $\bar{\sigma}$ (kg/cm ²)	Vol. strain $\frac{\Delta V}{V_o}$ (per-cent)	p_o (kg/cm ²)	Tot. vol. air at p_o $V_a + HV_w = n_o(1 - S_o - S_oH)$	$V_a + HV_w = n_o(1 - S_o - S_oH) + \frac{\Delta V}{V_o}$	$-p_o \times \frac{\Delta V}{V_o}$	Pore Pressure u (kg/cm ²)	Total stress σ (kg/cm ²)
(1)	(2)	(3)	(4)	(5)	(6) = (5) - (3)	(7) = (3) x (4)	(8) = (7) - (6)	(9) = (2) + (8)
1	0.4	-1.3	1.03	6.534	5.234	1.339	0.256	0.656
2	1.6	-3.0	1.03	6.534	3.534	3.090	0.874	2.474
3	3.2	-4.4	1.03	6.534	2.134	4.532	2.124	5.324
4	6.4	-6.0	1.03	6.534	0.534	6.180	11.573	17.973

The effective stress, computed values of pore pressures and total stress against compressibility are plotted in Fig.3.2.

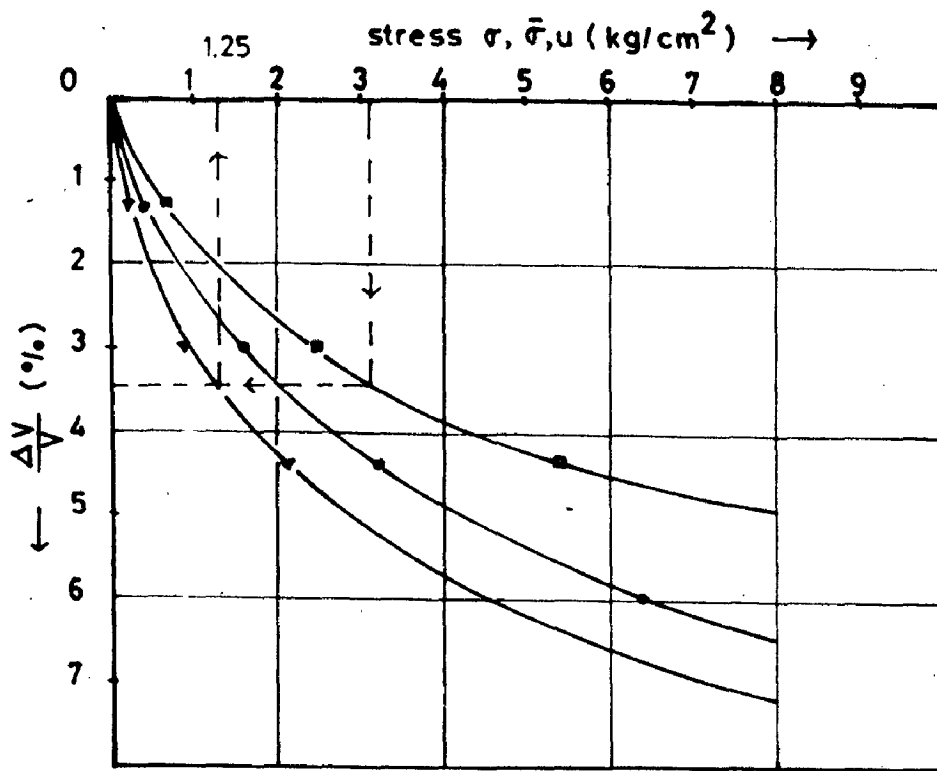


Fig.3.2. STRESS VS. VOLUME STRAIN

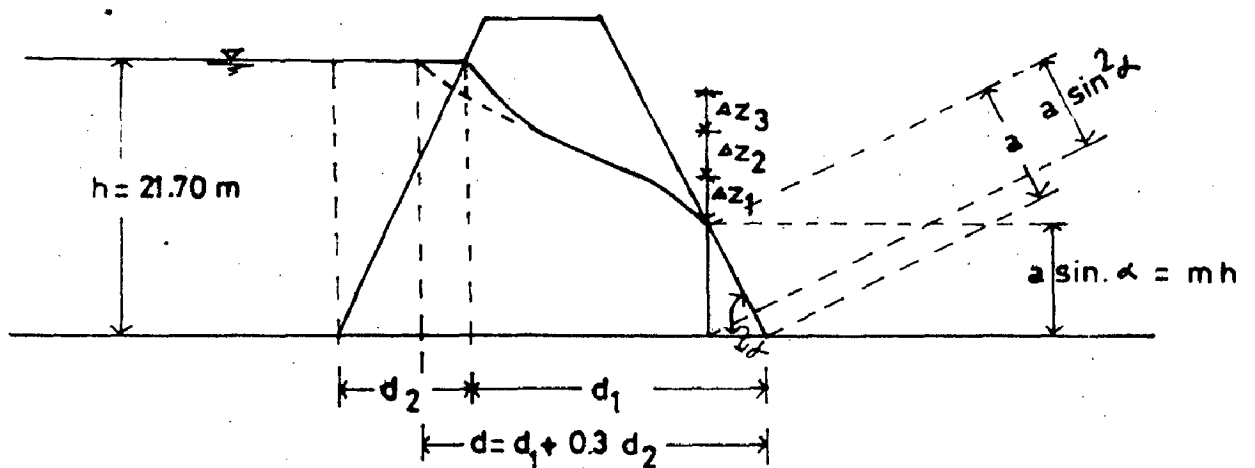


Fig.3.3. L. CASSAGRANDE METHOD

In the mid of December 1982, the fill elevation have reached + 51.00 m without any stoppage of construction, unit weight of the fill is 1.65 t/m^2 , therefore total stress $\sigma = (51 - 32) \times 1.65 = 31.35 \text{ t/m}^2 = 3.135 \text{ kg/cm}^2$.

The pore pressure correspond to total stress, $\sigma = 3.135 \text{ kg/cm}^2$ is 1.25 kg/cm^2 or 12.5 height of water column (Fig.3.2), while the maximum observed value measured by HP.4 is about 5 m, thus the estimated dissipation factor $= \frac{12.5 - 5}{12.5} = 0.60$. Since the corre material consists of high plasticity clay, this factor value is too high to be accepted, specially when time duration for dissipation is only 4 months and rate of construction is considerably high (3.25 m/month) i.e. the dam was raised at a constant speed of 10 cm/day.

3.1.2.3 Steady seepage pore pressures

During reservoir filling, the pore pressures recorded by tips no.HP.1, HP.2, HP.11 and HP.18 located in up-stream sand filter at El.+ 32.00 m, El.+ 40.00 m and El.+ 50.00 m respectively, have shown immediate response of readings. Correspond to the rise of reservoir water level without any appreciable phase lag, the pore pressures recorded by these tips, correspond to full reservoir level (El.+ 54.20 m) as shown in Fig.3.1.b, 3.1.c and 3.1.d respectively, indicating that filter zone is functioning very well. No pore pressures have been recorded by tips

no.HP.15 and HP.21 (Fig.3.1.c and 3.1.d respectively) located in downstream chimney filter. Pore pressures recorded for tips no.HP.6 and HP.7 (Fig.3.1.b) located in filter downstream of core, are of the order of 2.0 m (El. + 34.00 m) upto November, 1984, but thereafter the pressures have further increased by 2 to 3 m. At the end of December 1985, the excess pore pressures are of the order of 5 m. A steep rise from 2 m to 6 m was also noticed in both these tips during June and July 1984 through there was no increase in reservoir level during this period.

A study of pore pressures recorded by piezometers no.HP.3, HP.4 and HP.5 located at tier no.1 (El.+32.00 m), HP.8, HP.9 and HP.10 at tier no.2 (El.+35.00 m), HP.12, HP.13 and HP.14 at tier no.3 (El.+40.00 m), HP.16 and HP.17 at tier no.4 (El.+45.00 m) and HP.19, HP.20 at tier no.5 (El.+50.00 m), Fig.3.1.b, 3.1.c and 3.1.d respectively, embedded in the clay core zone, reveals that during impounding period, pore pressures are increasing simultaneously with the core material is behave as pervious material. Nil pore have been recorded by tip no.HP.22 (El.+54.00 m, Fig. 3.1.d) and the same is understandable as reservoir level is also at the level of tip installation.

A close look of the pore pressures recorded by tips embedded in clay core indicates that by and large, the steady seepage pore pressures developed follow the flownet pore pressures, when reservoir level has become constant

at El.+54.20 m from January 1984 onward, the readings of pore pressures for all tips embedded in clay core have also become almost constant.

A study of Fig.3.1.e showing the readings of vertical standpipes, indicate that as expected no significant pore pressures are developed in tips No.SP.3 to SP.5 located in downstream pervious shell zone. However pore pressures recorded for SP.2 embedded in clay core are of the order of El.+44.00 m, whereas the same for tip no.SP.1 are of the order of El.+41.00 m. In fact pore pressures should have been higher in tip no.SP.1 as compared to SP.2. Tip no.SP.1 is reported to be choked and hence its data cannot be accepted. The tip of SP.2 is at El.+37.00 m and thus the pore pressures recorded are of the order of 7.0m head of water. Hydraulic piezometer tip no.HP.10 located at El.+ 35.00 m is also almost at the location of SP.2 in the section. Pore pressure of the same order(El.+44.00 m) have been recorded by this HP.10 as well (Fig.3.1.c). Thus the observational data of hydraulic twin tube piezometers is also confirmed by the observation of Cassagrande type porous tube standpipe piezometers.

Fig.3.3.a and 3.3.b depict equi-pore pressure contours based on observational readings of hydraulic piezometers. Fig.3.3.a is just at the completion of filling, i.e. 10th January 1984 whereas Fig.3.3.b is for

readings taken after 15 months of attainment reservoir filling in March 1985. A study of these figures would indicate that the effect of anisotropy in the permeabilities of clay core, foundation treated by consolidation grouting and that of untreated foundation is noticeable. However there is practically no noticeable difference in between the contours drawn for observations taken after an interval of fifteen months. This again confirms that core is behaving as pervious fill with no time lag in recording of pore pressures.

3.1.2.4 Free surface line

Free surface line as obtained from twin tube hydraulic piezometers and that obtained by vertical stand pipe piezometer, is shown in Fig.3.3.c. From this figure it can be seen that free surface line obtained by twin tubing hydraulic piezometers is higher as compared to that obtained by vertical standpipe. Free surface line has also been determined using L.Cassagrande method as well as by electrical analogy method.

i) Determination of a phreatic line using L.Cassagrande approach :

This method is based on the assumption that the foundation layer is impervious, though here it is not so, because the foundation consists of medium to heavy weathered buff breccia and tuffaceous sandstone having permeability of the order of 7×10^{-5} cm/sec to 8.4×10^{-2} cm/sec. Nevertheless

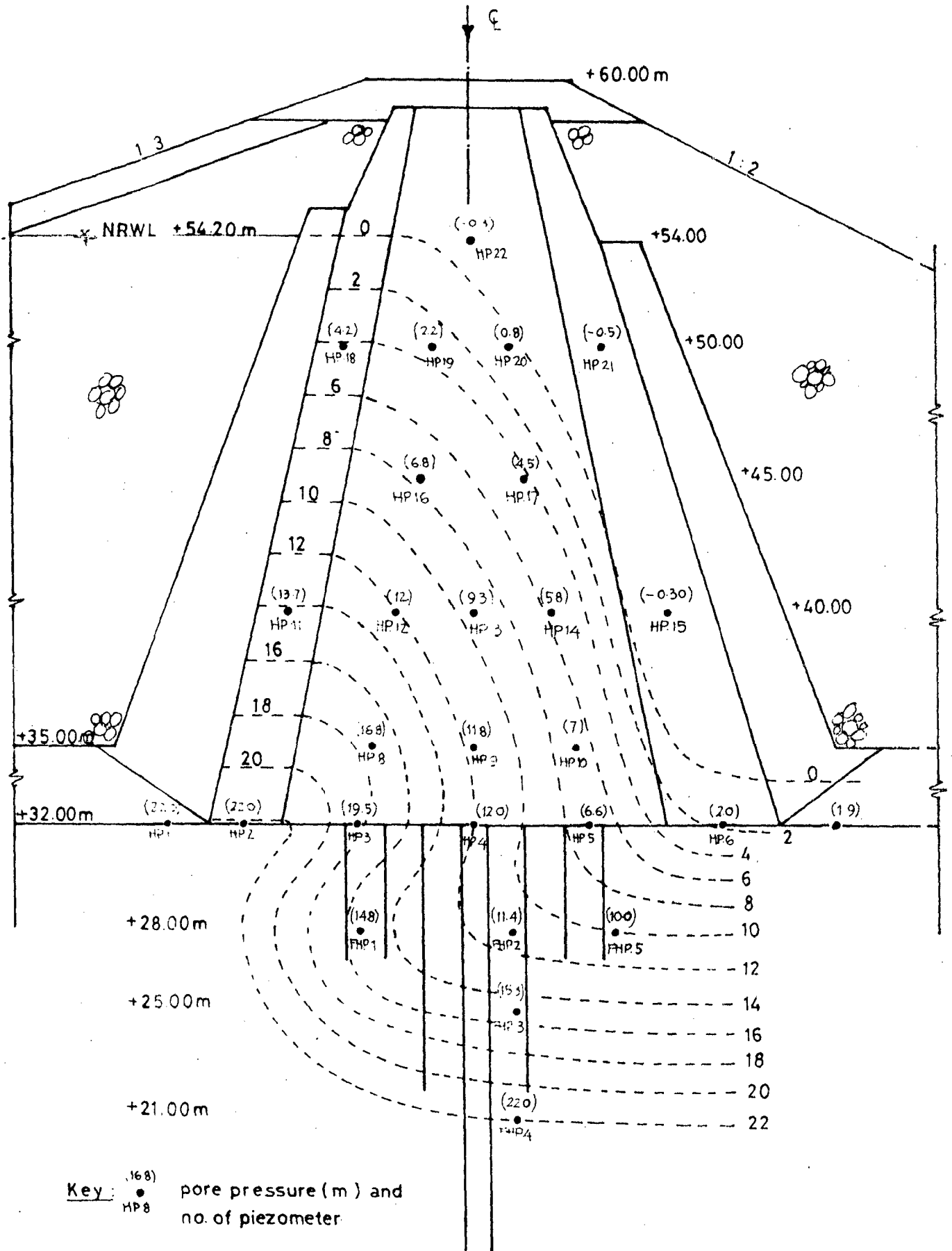


Fig 3.3^a EQUI-PORE PRESSURE CONTOUR AT STA. 23⁺¹⁵
(Based on measurement on 10 January 1984)

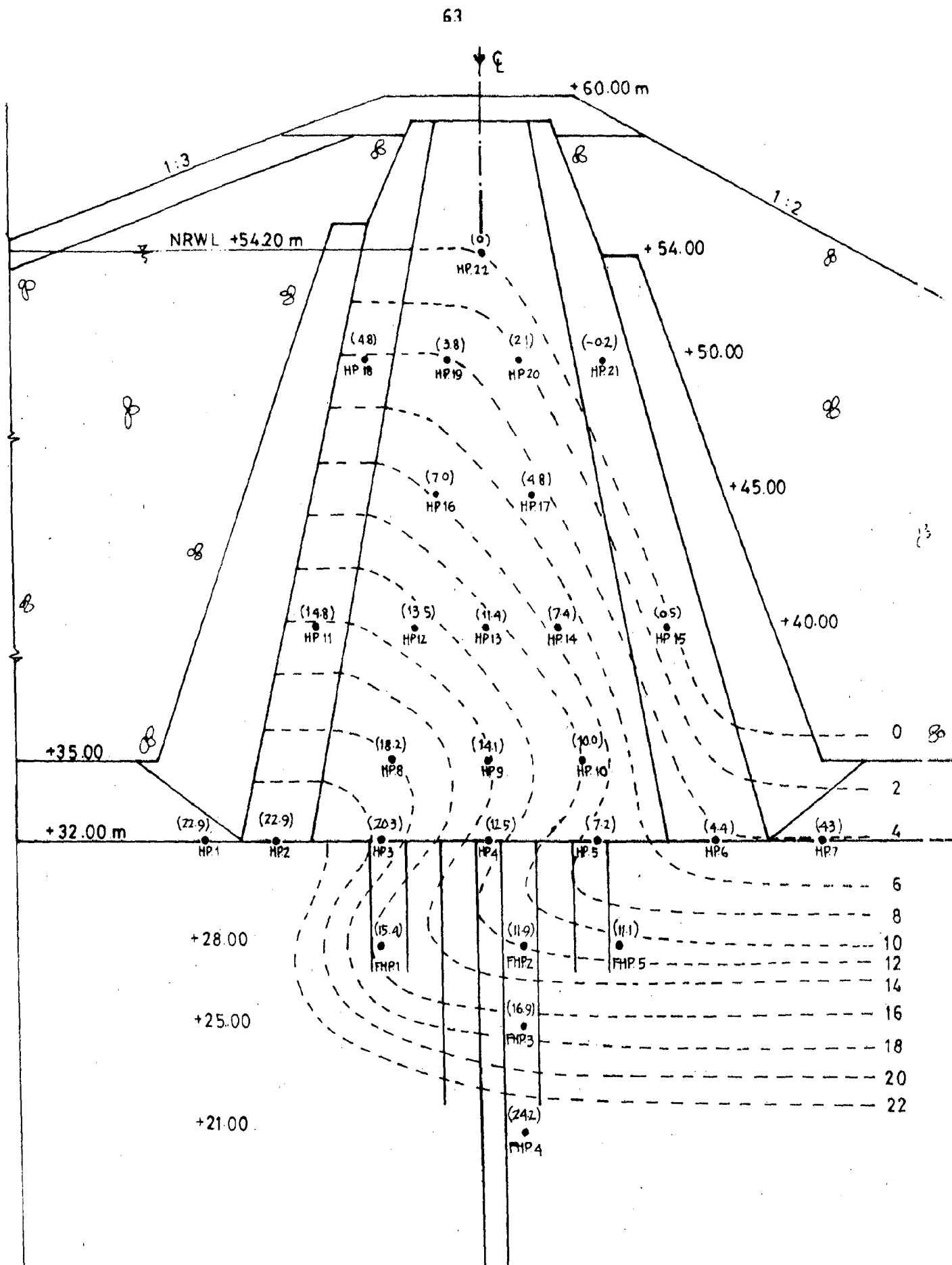


Fig. 3.3^b EQUI-PORE PRESSURE CONTOUR AT STA. 23⁺¹⁵
 (Based on measurement on March 1985)

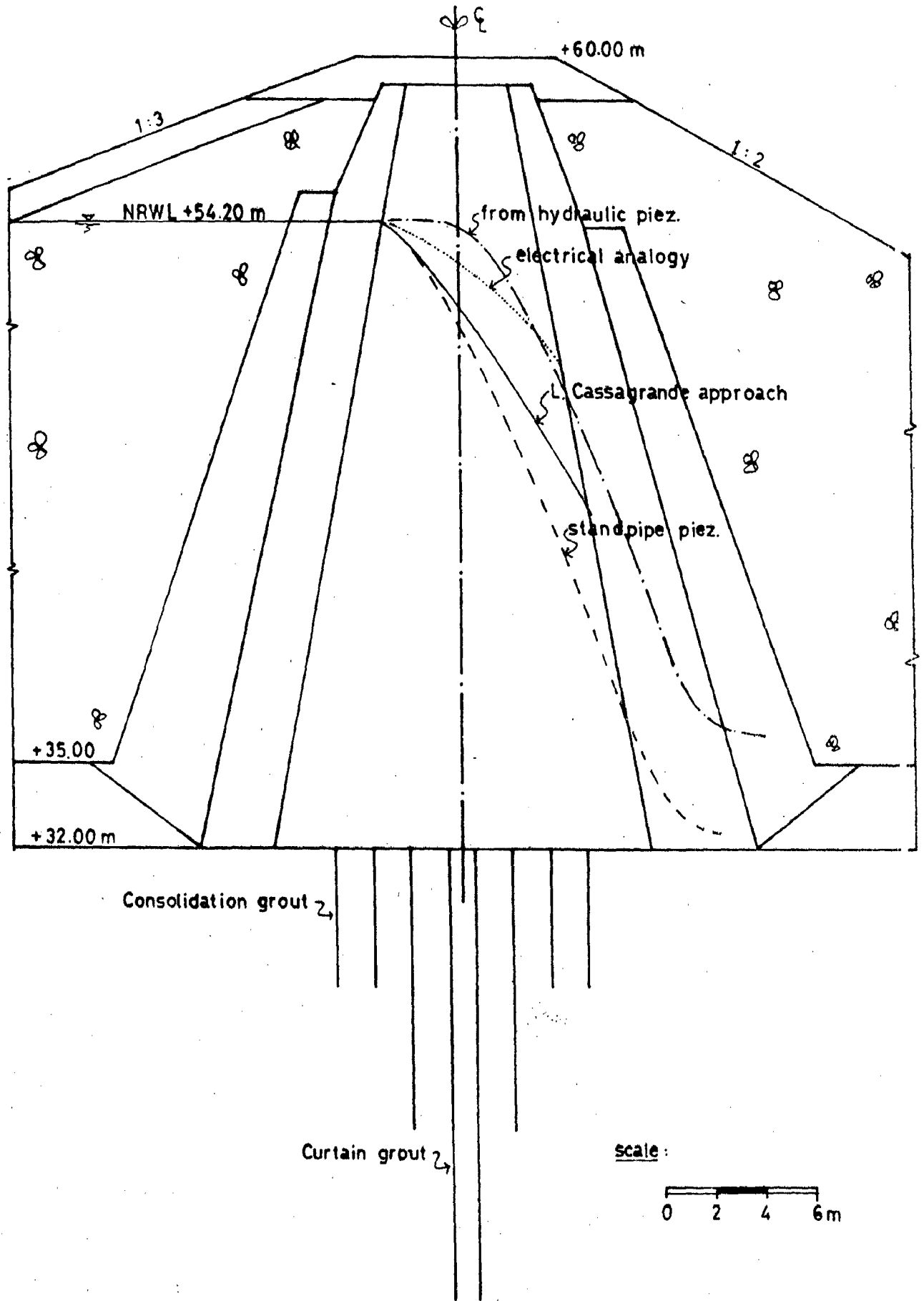


Fig.3.3^c DETERMINATION OF PHREATIC LINE

the free surface line by L.Cassagrande was drawn as shown in Fig.3.3.# and its calculation in briefs are shown as under :

$$d = d_1 + 0.3d_2 = 10.50 + 0.3(4.5) = 11.85 \text{ m}$$

$$h = 21.70 \text{ m}$$

$$\alpha = 79^\circ$$

From G.Gilboy's Chart, $m = 0.55$

$$\frac{d}{h} = \frac{11.85}{21.7} = 0.546$$

$$mh = a \sin \alpha = 0.55 \times 21.70 = 11.94 \text{ m say } 12 \text{ m}$$

$$a = \frac{12}{\sin 79} = 12.22 \text{ m}$$

$$a \sin^2 \alpha = 12.22 \sin^2 79 = 11.78 \text{ m}$$

$$\text{By taking } \Delta Z_1 = \frac{11.78}{3} = 3.92 \text{ m}$$

and $\Delta Z_1 = \Delta Z_2 = \Delta Z_3$, hence the phreatic line can be drawn.

- ii) In performing electrical analogy model, an average permeability of 1×10^{-3} cm/sec prior to grouting and $k = 6 \times 10^{-4}$ cm/sec after grouting are taken by assuming that the layer is isotropic. The free surface line is drawn by trial such that at surface, the pressures are zero, this is also shown in Fig. 3.3.c. Again, it is too far to the fact that the foundation layers are non-homogeneous, because the soil properties change considerably.

iii) It can be seen that hydraulic piezometers have shown the highest position to free surface followed by electrical analogy method, whereas standpipe readings have given the lowest value. L.Cassagrande method gives free surface line in between standpipe and twin tube hydraulic piezometer readings. The results obtained by electrical analogy method are more or less nearer to twin tube hydraulic piezometer observed pore pressures and hence electrical analogy method is preferable in case of anisotropic foundation.

3.1.2.5 Drawdown pore pressures

Observations of drawdown/^{pore}pressures are not available, because the drawdown of reservoir itself has not yet occurred during last two years because of delay in the construction of channels.

However, the estimation of drawdown pore pressure was carried out using Bishop's approach for compressible fill, since the core material consists of high plasticity reddish brown clay, classified as CH-group.

$$u = \gamma_w [h_c + h_r(1-n_s) - h']$$

Assuming that the core material is fully saturated and the reservoir level + 54.20 m is to be drawn to the elevation + 35.00 m, drawdown pore pressures for some tips

located in core zone have been shown in Table 3.3. When actual drawdown will take place, it will be of interest to see whether fill behaves as compressible fill or incompressible permeable fill as for steady seepage pore pressures, it has behaved as pervious fill.

Table 3.3 : Drawdown Pore Pressures by Bishop's Method

Sl. No.	Peiz. No.	h_c (m)	h_r (m)	h' (m)	u (m)
1	HP.12	14.2	-	1.8	13.2
2	HP.13	12.6	-	2.2	10.4
3	HP.14	10.5	-	3.0	7.5
4	HP.16	8.6	-	1.2	7.4
5	HP.17	6.2	-	1.2	5.0
6	HP.19	3.6	-	1.0	2.6
7	HP.20	1.5	-	0.5	1.0

3.2 VERTICAL AND HORIZONTAL MOVEMENT

3.2.1 Vertical Movement (Settlement)

3.2.1.1 Presentation of Observational data

The frequency of observation on vertical extensometer for measuring settlement of core embankment is carried out once a week in loading test period, once a month in stabilisation period and twice a year in maintenance period. The installation date of each element in various elevation is shown in Fig.2.3.b.

The measurement of settlement can be done by lowering a Reed switch probe into the access tube. When the probe enters the magnetic field produced by a target (magnetic plate), an audible signal is emitted at ground level. Measurements made on a steel tape may then be related to a datum ring magnet fixed in the rock foundation at El. + 30.041 m.

3.2.1.2 Analysis

(a) Observed settlement

A study of Fig. 3.1.d showing settlement plates no.1 to 4 which are embedded at El. + 32.773 m, + 37.439 m, + 41.924 m and + 46.736 m respectively, indicates that during construction period (August to December 1982), the settlement recorded vary from 0.5 cm to 2.5 cm. The smallest value was recorded by plate no.1 and the largest value by plate no.4. No significant values of settlement were recorded by plates no. 5 and 6 from their installation in

February and March 1983 until October 1983 where reservoir filling started. At the end of construction in October 1983, the settlement of the order of 8 cm to 10.5 cm was recorded by plates no.1, 2, 3 and 4.

During reservoir filling from October to December 1983, a steep rise in settlement is recorded by almost all plates. In case of plate no.4, the settlement increase from 10 cm to 27 cm. For plate no.5 and 6 increase upto end of December 1983 was of the order of 12 cm to 13 cm. Plate no.1, 2, and 3, indicated rise during this period from 8.5 cm to 10 cm, 9 cm to 20 cm and 10 to 23 cm respectively. This shows that depending upon location of plate, maximum settlement has been recorded during reservoir filling and which is of the order of 13 cm to 17 cm for plates located in the upper height of dam. Non-recording of settlement by top plates no. 5 and 6 during construction period (March - September 1983) may be due to some arching action of core by adjoining shell zones which might have reduced during reservoir filling, because of lubrication due to saturation and hence during reservoir filling, settlement is recorded by these plates as well. It is interesting to note that for plates no.1, 2, 3 and 4, settlement after completion of filling (December 1983) upto October 1985 has increased only by about 2 cm to 3 cm, whereas in case of plates no. 5 and 6, the settlement recorded in post-filling period is of the order of 5 cm to 6 cm. This shows that from the date

of starting reservoir filling, the total settlement recorded by plates no. 4, 5 and 6 is of the same order i.e. about 19 cm to 20 cm. It may further be noted that beyond April 1984, settlement recorded is practically negligible, so here settlements are taking place almost simultaneously or with little phase lag.

(b) Terzaghi's one-dimensional consolidation settlement

The estimation of settlement of clay core was also done by means of Terzaghi's one-dimensional consolidation theory, using following consolidation test data :

Wet density, $\gamma_m = 1.65 \text{ t/m}^3$

Compression index, $C_c = 0.118$

Initial void ratio, $e_0 = 1.407$

Coefficient of consolidation, $C_v = 6 \times 10^{-3} \text{ cm}^2/\text{sec.}$

The calculation of settlement was done by assuming top elevation of clay core at + 56.0 m, where top settlement plate no.6 was installed. The height of clay core is divided into 4 m lift each and the calculations are tabulated in Table 3.4.

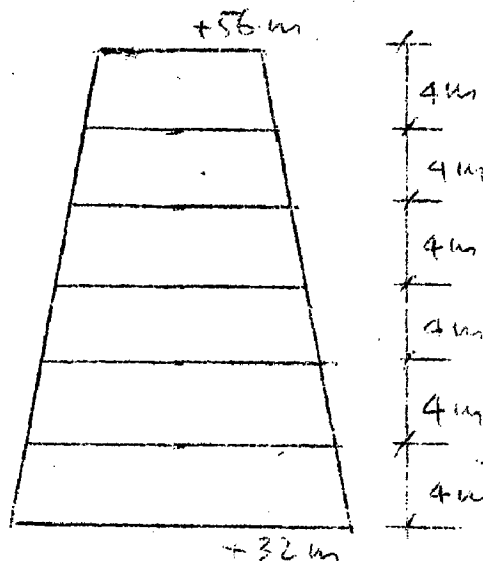


Fig. 3.4

Table 3.4 : Settlement Calculation by Terzaghi's 1-D Consolidation Theory

Sl. No.	H (m)	σ_0 (t/m ²)	σ_1 (t/m ²)	$\log \frac{\sigma_1}{\sigma_0}$	$S_c = \frac{H}{1+e_0} C_c \log. \frac{\sigma_1}{\sigma_0}$ (m)
1	4	3.3	9.9	0.477	0.059
2	8	6.6	13.2	0.301	0.118
3	12	9.9	16.5	0.222	0.130
4	16	13.2	19.8	0.176	0.138
5	20	16.5	23.1	0.146	0.143
Total					0.588

$$T_v = \frac{C_v \cdot t}{d^2}, \text{ for half layer, } d = 20 \text{ m} = 2000 \text{ cm}$$

$$T_v = \frac{6 \times 10^{-3}}{2000^2} t \quad \text{or } t = 6.67 \times 10^8 T_v = 21.15 T_v \text{ (Years)}$$

Table 3.5

Sl.No.	U	T_v	S_c (cm)	Time (years)	Remarks
1	0.10	0.008	0.059	0.169	
2	0.15	0.016	0.088	0.338	
3	0.30	0.070	0.176	1.481	
4	0.40	0.130	0.235	2.750	
5	0.50	0.190	0.294	4.018	
6	0.90	0.848	0.530	17.935	

Fig.3.5 showing the comparison between computed settlement and observed settlement. It is clear, during construction period t_c , the corrected settlement curve is very close to the observed curve, but after filling of reservoir the observed curve dropped immediately corresponding to the rise of reservoir level, indicates that saturation of clay core is faster than that of Oedometer sample as expected earlier. Again it shows that the core is behave as pervious material. Pore pressure reading and free surface also confirms that saturation of clay core is taking place simultaneously with reservoir filling.

It is also seen that total observed settlement is about 30 cm whereas theoretically calculated settment is 59 cm. This shows that actual observed settlement is only 50 percent of anticipated settlement. This may be due to possible inaccuracies in determination of soil properties such coefficient of consolidation in laboratory. Quick response to settlement may be due to two dimensional effect in prototype.

3.3.2 Horizontal movement

3.2.2.1 Presentation of Data

The vertical extensometer above is combined with inclinometer for measuring horizontal movement using aluminium tube formed with four grooves around its circumference.

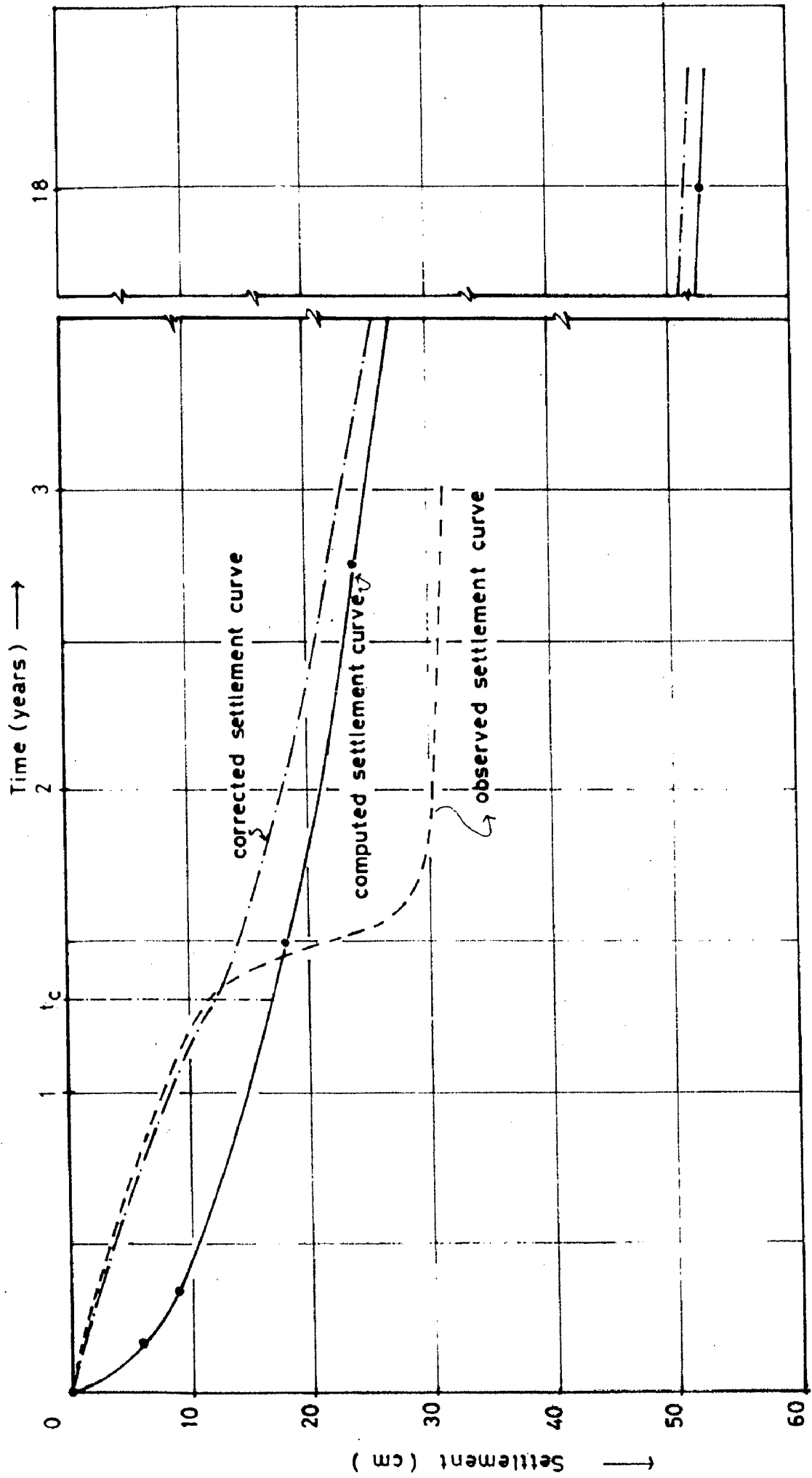
Two grooves are aligned in the upstream and downstream direction and in the diversion canal and spillway direction for the others. By positioning a torpeda connected to a digital read out unit at 0.5 m interval in the aluminium tube, various horizontal deformation at various interval of depth can be recorded.

Fig.3.1.f shows a plot in between observed displacement and depth measured initially on 16 November 1982 on the completion of dam and continued untill 25 September 1985. During filling of reservoir period at El. + 54.20 m, maximum displacement of 4.1 cm (5.7 cm - 1.6 cm) in diversion canal direction at about 14 m depth was recorded on 25 September 1985 and 6 cm (4 cm + 2 cm) deformation in downstream of dam direction at about 17 m depth were also measured on 29 October and 27 March 1984.

3.2.2.2 Analysis

A study of Fig.3.1.f showing displacement of dam body in two alignment, i.e. spillway diversion canal alignment and upstream - downstream alignment respectively. The figure tells that at the beginning of reservoir filling in October 1983, the core moved to diversion canal diversion and downstream alignment. The deformation then altered to spillway direction in April 1984 but still in downstream direction.

Fig. 3.5. OBSERVED AND COMPUTED TIME SETTLEMENT CURVE



This movement continued to diversion canal direction until the maximum movement of 4.1 cm was attained in September 1985. Otherwise this displacement was changed to upstream direction at the same time. It is indicated, that after construction but prior to reservoir filling, the dam might reach a state of equilibrium and however might be abruptly altered during reservoir storage.

A close look of Fig.3.1.f indicates that height wise, we have three distinct regions so far as horizontal movement is concerned viz. one is for top of dam to 4 m depth, second is 4 m depth to 10 m depth and third is 10 m depth to the bottom most anchor point in foundation. So far as second zone (4 - 10 m depth from top) is concerned, there is practically no movement either along the axis or perpendicular to dam axes. In first region (top 4.0 m), downward movement of about 1.5 cm is recorded after 4 months of reservoir filling but it has returned to normal position by Sept. 1985 conforming that there is no downward movement. Similar is the trend for movement along dam axis in the region. However, in region 3 (10 m to foundation) maximum downward movement of the order of 4 cm from normal, have been recorded after ten months of filling (29th October 1984) which has subsequently reduced to 2.0 cm after one year (29th Sept. 1985). For movement along dam axis in this region, the movement towards diversion canal is increasing with time and has

already attained a value of the order of 6 cm deflection. Normally no lateral movement should be expected. The behaviour of readings in third zone needs still investigations.

3.2.3 Surface displacement

The measurement of surface monuments placed at the crest and slopes of dam were done by means of theodolite, after completion of the dam. The data is not available because of the impossibility of ascertaining whether movement is deep seated or superficial and because the magnitude of motion is normally within the limit of error of the measuring method.

4. EXPERIMENTAL SET-UP

4.1 GENERAL

Solutions to seepage flow problems in two dimensions or three dimensions can be obtained with electrical analogy models having similar geometric shape corresponding to structures and soil profile through which the water flows. The seepage medium is replaced by an electric conductor and the boundary conditions are established by applying electric potentials at the source and exit of flow.

The drop in potential across the model simulates the drop in water head in the prototype and is measured with a voltmeter. The model acts as two arms of a wheat stone bridge circuit and a calibrated slide wire potentiometer as the other two arms. To determine a line contour of equal potential, the potentiometer is adjusted to percentage of the total voltage drop and the probe of a galvanometer is used to find the corresponding balance points on the model.

Changes in the coefficient of permeability of the soil zones in the seepage analog are simulated by changes in the electric conductivity coefficient in the model. For seepage problem having zones of different permeabilities, three zones are to be represented in the model with different electric conductivity in the ratios of field permeability anticipated in prototype.

4.2 ANALOGY APPROACH

Darcy's law governing the flow of water through soils is analogous to the Ohm's law for flow of electrical current through a conductor.

Darcy's law $q = K.i.A$, where $i = H/L$

Ohm's law $I = \sigma \frac{U}{L} A$

where

K = coeff. of permeability of soil

H = hydraulic head

A = unit area

L = unit length

σ = coeff. of conductivity of conductor

U = voltage drop

The flow pattern of water as well as that of current can both be known by the Laplace equation which for an isotropic, two-dimensional medium is

$$\frac{\partial^2 \phi}{\partial x^2} + \frac{\partial^2 \phi}{\partial z^2} = 0$$

ϕ represents the hydraulic potential in case of water flow and the electrical potential (U) in case of current flow.

$$\frac{\partial^2 u}{\partial x^2} + \frac{\partial^2 u}{\partial z^2} = 0$$

The analogy between the seepage and electric current is given below. (After Aravin and Numerov, 1965).

Sl. No.	Seepage through porous medium	Current flow through the conducting medium
1.	Seepage discharge, q	Current intensity, i
2.	Flow line	Current line
3.	Coeff. of permeability, K	Coeff. of conductivity, σ
4.	Piezometric head	Electric potential
5.	Equipotential line, $h = \text{constant}$	Equipotential line, $u = \text{constant}$
6.	At pervious boundary $\frac{\partial h}{\partial n} = 0$	At insulating surface, $\frac{\partial u}{\partial n} = 0$
7.	Where n is normal to the boundary	Where n is normal to the surface
8.	Darcy's law, $q = K \cdot i \cdot A$	Ohm's law, $I = \sigma \cdot \frac{U}{L} \cdot A$
9.	Laplace eqn. $\frac{\partial^2 \phi}{\partial x^2} + \frac{\partial^2 \phi}{\partial z^2} = 0$	Laplace eqn. $\frac{\partial^2 U}{\partial x^2} + \frac{\partial^2 U}{\partial z^2} = 0$
10.	Seepage velocity, v	Current velocity, i
11.	The integral of Laplace eqn. $h = f(x, z)$	The integral of Laplace eqn. $u = f(x, z)$

Three methods of electrical analogy commonly used are :

- Conductive Tray Method
- Beltronix Analog Plotter and
- Conductive Paper Method

The conductive Tray Method is applicable for stratified soil layer or non-homogeneous zones with different permeabilities, while the second and the third are suitable for homogeneous layers. In the case of Rarem Dam having different permeabilities of clay core, consolidation grout zone and foundation, the conductive tray method was adopted. Coefficient of permeabilities of zones to be considered in experiment are shown in Table 4.1.

Table 4.1 : Conductivities of Different Zones of Materials

Sl. No.	Zone	Coeff. of permeability, K (m/s)	Relative K	Conductivity (micro ohms)
1.	Clay core	6×10^{-6}	1 K	5.0×10^2
2.	Consolidation grout	5.6×10^{-4}	100 K	5.0×10^4
3.	Foundation	1×10^{-3}	200 K	10.0×10^4
4.	Downstream filter	1.8×10^{-3}	300 K	15.0×10^4

4.3 CONDUCTIVE TRAY METHOD

4.3.1 Model

The conductive tray is a shallow tank with flat bottom constructed of an insulating material which contains electrolyte. The bottom and the sides of the tray are made of 5 mm

thick perspex glass. The lateral dimensions were taken 3 times of the reservoir water head that boundary conditions do not affect the results. The joint between the bottom and the sides is made water tight by using chloroform.

Following boundaries were simulated in the model.

(i) The foundations of Rarem dam are permeable to infinite depth. The depth has been limited to three times head of water in the model. Laterally the extent of model is also three times water head both upstream and downstream of dam so as to minimize the boundary effect.

(ii) Upstream Dam Face :

It is a water retaining boundary on which the hydraulic potential is constant. This permeable boundary is upstream slope and also horizontal upstream extension upto 3 H in reservoir. It has been simulated by a continuous perspex glass to which a continuous copper plate is also fixed and 100 percent potentials applied.

(iii) Free Surface

Along this surface, the pressure is atmospheric, and therefore $\phi = z$, where z is position of head. This is determined by trial and error and is represented by plastic clay in dam body. Along the downstream face of core, potentials corresponding to height were given through wires.

(iv) Downstream boundary

Downstream of dam, again copper sheet was attached to perspex sheet and zero potentials were given to it.

(v) Interfacing boundaries of different permeability

There are primarily three permeability zones viz. core zone, consolidation grouting zone and foundation zone. To allow flow of current through these zones, copper loops situated at a distance of 5 mm and on perspex sheets dividing the zones were used.

The model set-up is shown in Fig.4.3.

4.3.2 Electrolytes

The conductivities of four different electrolytes as indicated in Table 4.1 were obtained by mixing sodium chloride in distilled water or tap water depending the conductivity. Distilled water was used for clay core having low conductivity where as tap water for other zones, having comparatively high permeabilities.

Mandavia, (1984) reported that the conductivity of electrolyte changes with temperature, evaporation and contamination from atmospheric impurities.

In the case of Rarem dam model, in case of electrolyte prepared in distilled water, the conductivity changed by 1.5 percent and 4.6 percent when placed in open air and

covered condition respectively. However the trend was reversed for electrolyte prepared in tap water. For this case, the change in conductivity was 3.9 percent in case of open air and 2 percent for covered beaker. Though it is not explicitly proved by tests, it will be advantageous to keep the electrolyte covered. Nevertheless the change in conductivity in 24 hours is of very low order and can be accepted.

4.3.3 Instrumental set-up

- i) Power supply circuit comprising
 - a) Power source
 - b) Voltage-control devices
 - c) The devices setting up the potentials on the various model boundaries.

The power source was obtained from electric mains, having 220 V at a frequency of 50 cycles/sec.

The voltage-control device includes the step down transformer where 220 V can be stepped down to 25 V. The current frequency was raised to audio range by audio oscillator.

- ii) Measuring circuit

The diagram of the circuit is shown in Fig.4.3.b. The model is divided into two parts by an equipotential line with resistances R_1 and R_2 . The moving contact key of potentiometer, divides the potentiometer wire into parts with

the resistances r_1 and r_2 . In the balance condition

$$\frac{r_1}{r_2} = \frac{R_1}{R_2}$$

Hence,

$$\frac{r_1}{r_1 + r_2} = \frac{R_1}{R_1 + R_2} = \frac{u_1 - u_3}{u_1 - u_2}$$

where,

u_1 = upstream potential in volts

u_2 = downstream potential in volts

u_3 = potential at any point

Since the resistance of the calibrated potentiometer wire is proportional to its length, by denoting the lengths of the sections with the resistances r_1 and r_2 by l_1 and l_2 respectively :

$$\frac{l_1}{l_1 + l_2} = \frac{u_1 - u_3}{u_1 - u_2}$$

Therefore, when magic eye indicates null position, the ratio between the length of the left hand side of the potentiometer wire and the total length of the wire is equal to the ratio between the potential drop in the shaded part of the model to the total potential drop over the whole model.

Mandavia, (1984) also observed the cause of the errors such as mechanical error, polarization, effect of surface tension, probe effect and non-uniformity of electrolyte. According to Karplus (1958), an accuracy of ± 2 percent can be considered as an adequate for most engineering purposes.

Fig. 4.3.^a ELECTRICAL ANALOGY - CONDUCTIVE TRAY MODEL
(not to scale)

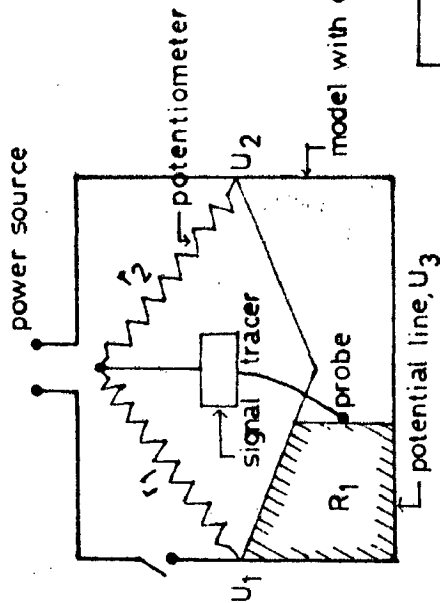
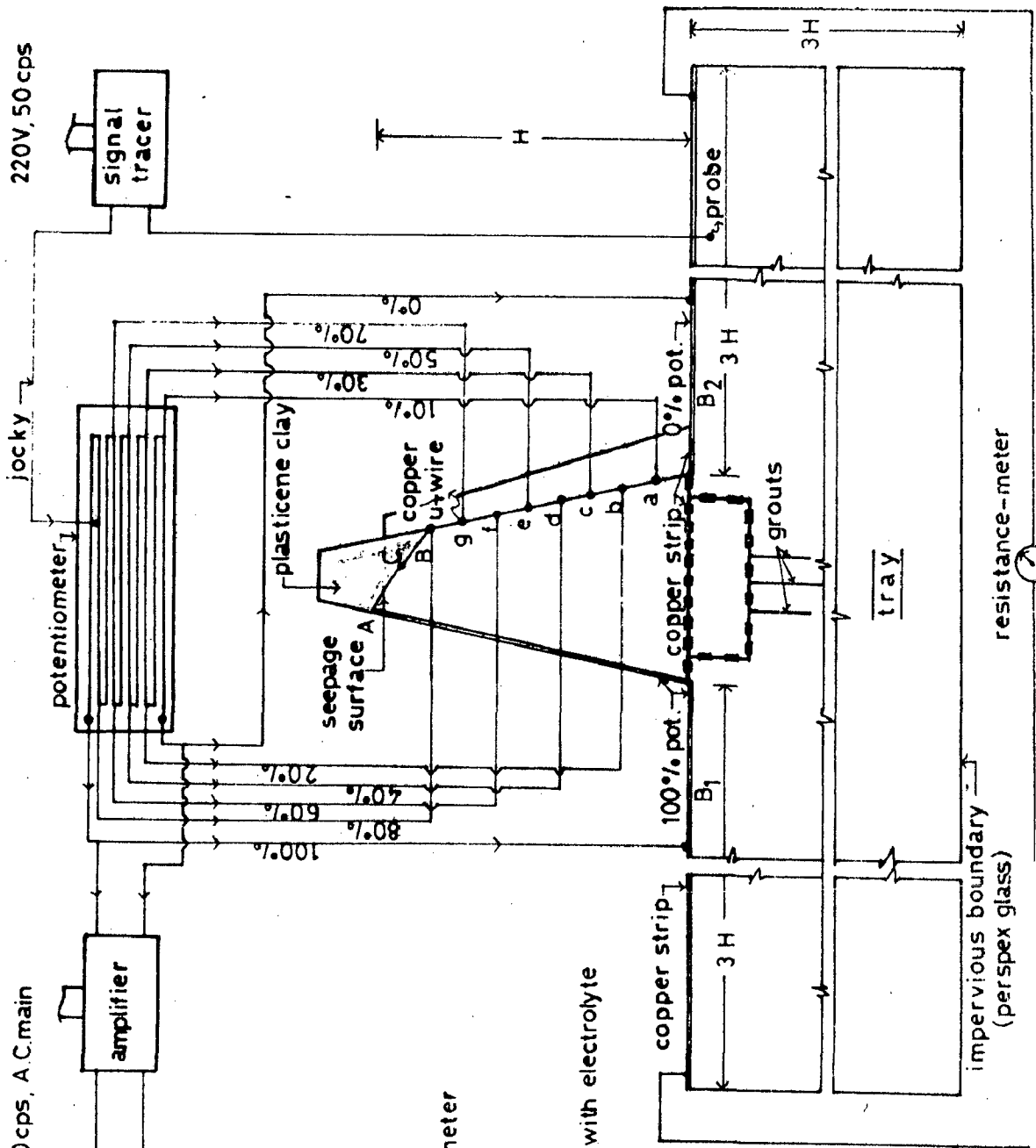


Fig. 4.3.^b MEASURING CIRCUIT

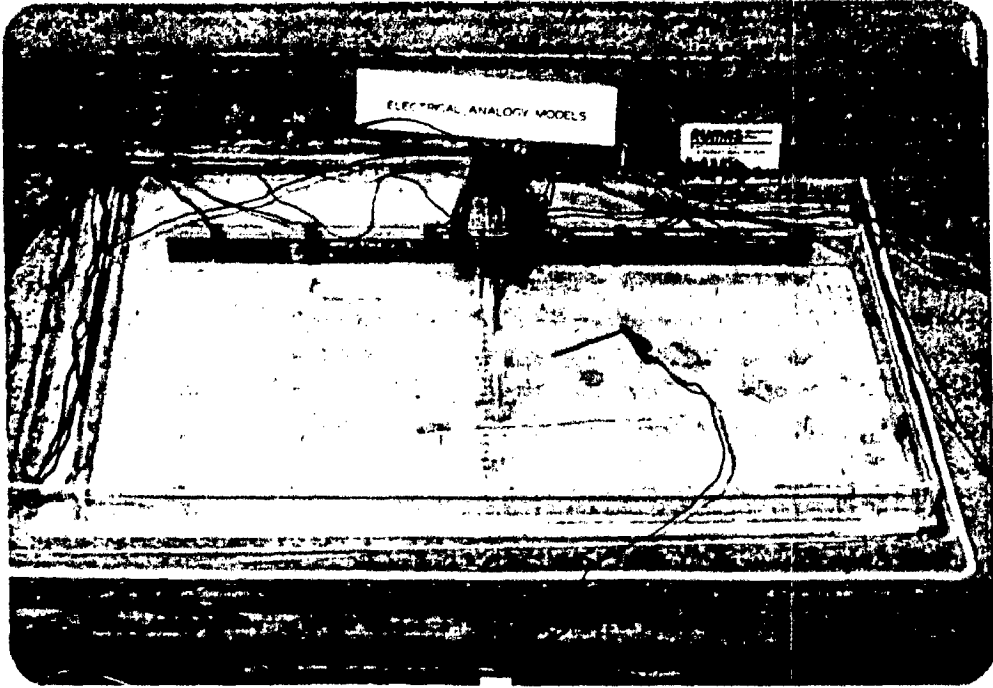


Photo 4.1. Conductive tray model

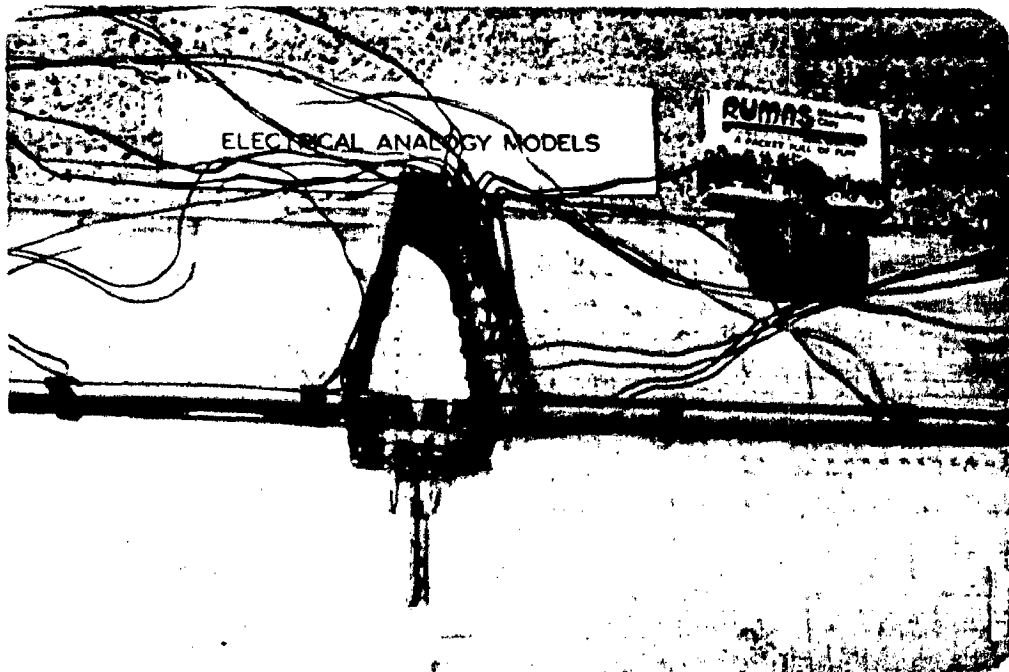


Photo 4.2. Simulation of core and grout in detail

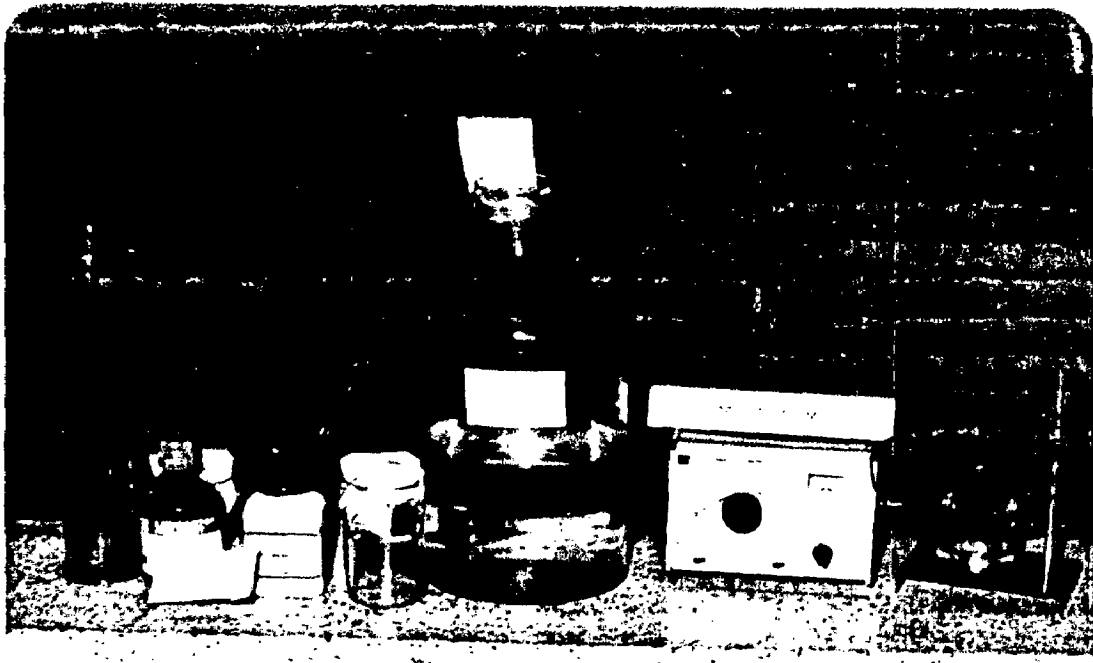


Photo 4.3. Electrolyte and Conductivity meter

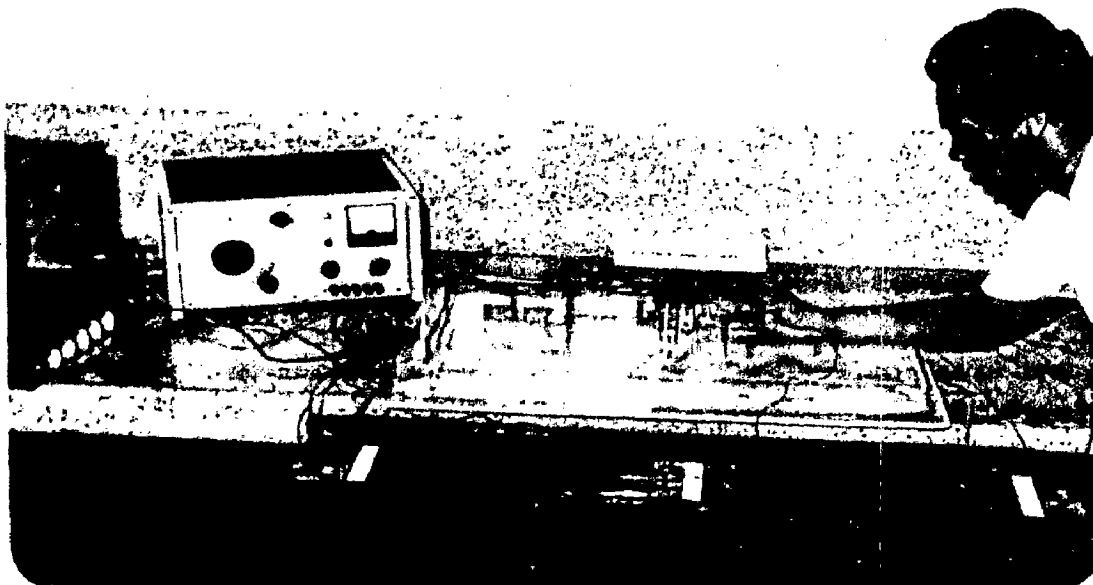


Photo 4.4. Instrument set-up - Experiment in progress

5. COMPARISON AND ANALYSIS OF OBSERVED AND LABORATORY TEST DATA

5.1 Cases Studied

Potentials and resistances offered by the electrolytes, representing permeability of different zones were observed on two dimensional electrical analogy-conductive tray model for six conditions of grouts-

- | | | |
|----|---|---|
| a) | Grouts curtains with 100 percent efficiency | (perspex sheets representing grout curtain were used) |
| b) | Grouts curtain with 75 percent efficiency | (25 percent of perspex sheets representing grout curtain were perforated). |
| c) | Grouts curtain with 50 percent efficiency perforated | (50 percent of area of perspex sheets representing grout curtain were perforated) |
| d) | Grouts curtains with 25 percent efficiency perforated | (75 percent of area of perspex sheet representing grout curtain were perforated) |
| e) | Curtain grout completely ineffective | (no perspex sheets representing grout curtain) |

The entire grouts viz. both consolidation and curtain grouting completely ineffective.

5.2 Presentation of Experimental Data

5.2.1 Pore Pressures

The variation of potential in the various selected measurement points of each condition are plotted in Fig.5.1a to 5.1f and based on these values, the equipotentials have been drawn.

5.5.2 Stability of Electrolyte

The values of conductivity of the electrolytes at the beginning of test and the end of test are tabulated below - (Table 5.1).

Obviously, it is seen from the Table 5.1 that the smaller the conductivity value, the more sensitive the electrolyte will be, the maximum sensitivity of electrolyte is

$$\frac{(5.4 - 5.0)10^2}{5.4} \times 100 \text{ percent} = 7.4 \text{ percent}$$

It can be concluded that during experimentation, the electrolyte has remained practically stable even though the variation in conductivity is quite large (of the order of 300 times).

5.3 Comparison and Analysis

Percentage potential at any point under various conditions of the grouts, can be estimated at any point from the data plotted in Fig. 5.1(a) to 5.1(f). Our interest is to compare the observed potentials for piezometers FHP1 to FHP5 with various conditions of testing. Observed pore pressure values for these five piezometers together with percent potentials observed on the model for six cases of grout efficiencies, are shown in Table 5.1. The relationship of percent grout efficiency and percent pore pressures as observed on the model is shown in Fig. 5.2. for five foundation piezometers.

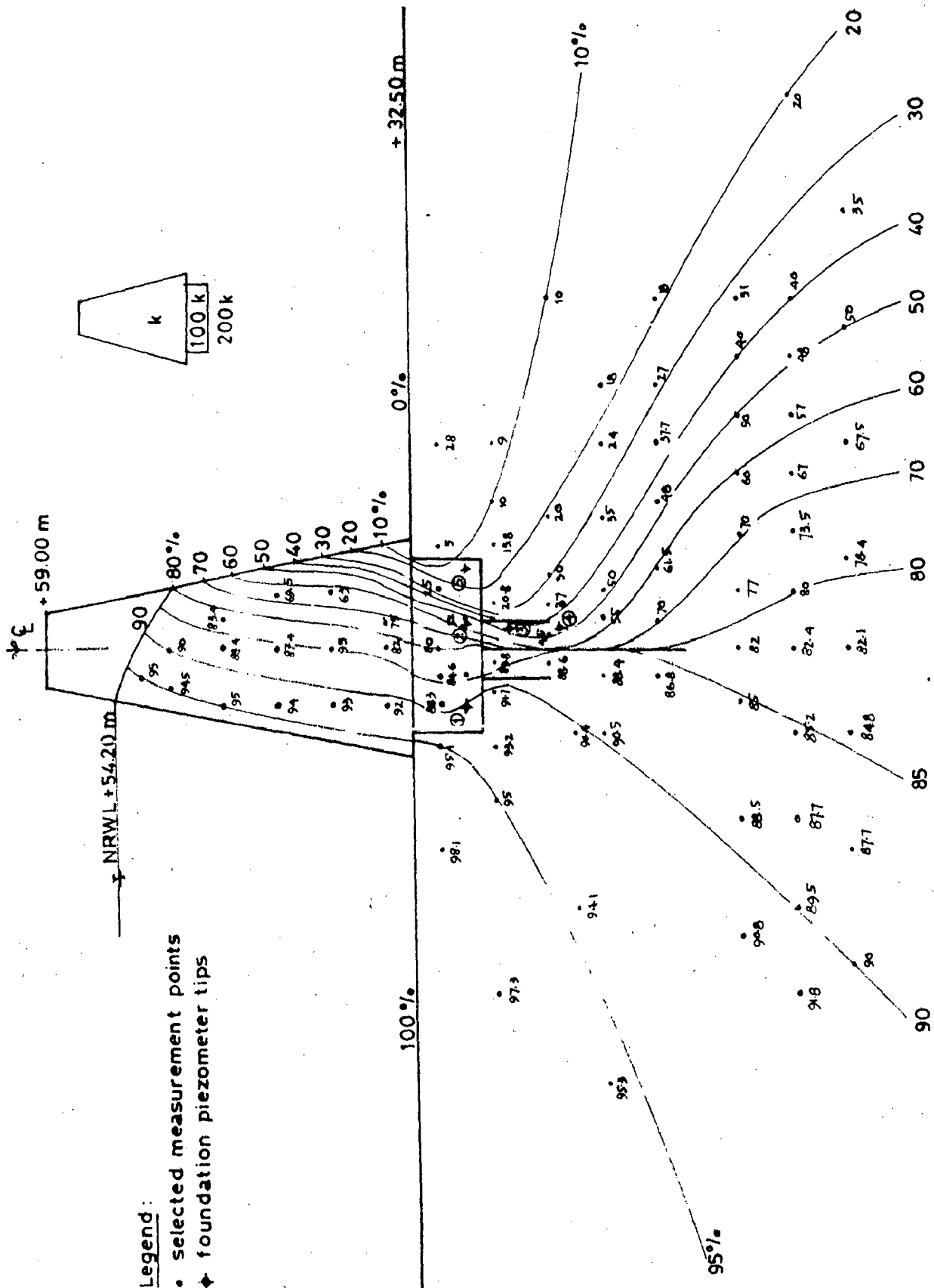


Fig. 5.1^a EQUIPOTENTIAL LINES FOR 100% EFFICIENCY OF GROUTS
Scale 1:400

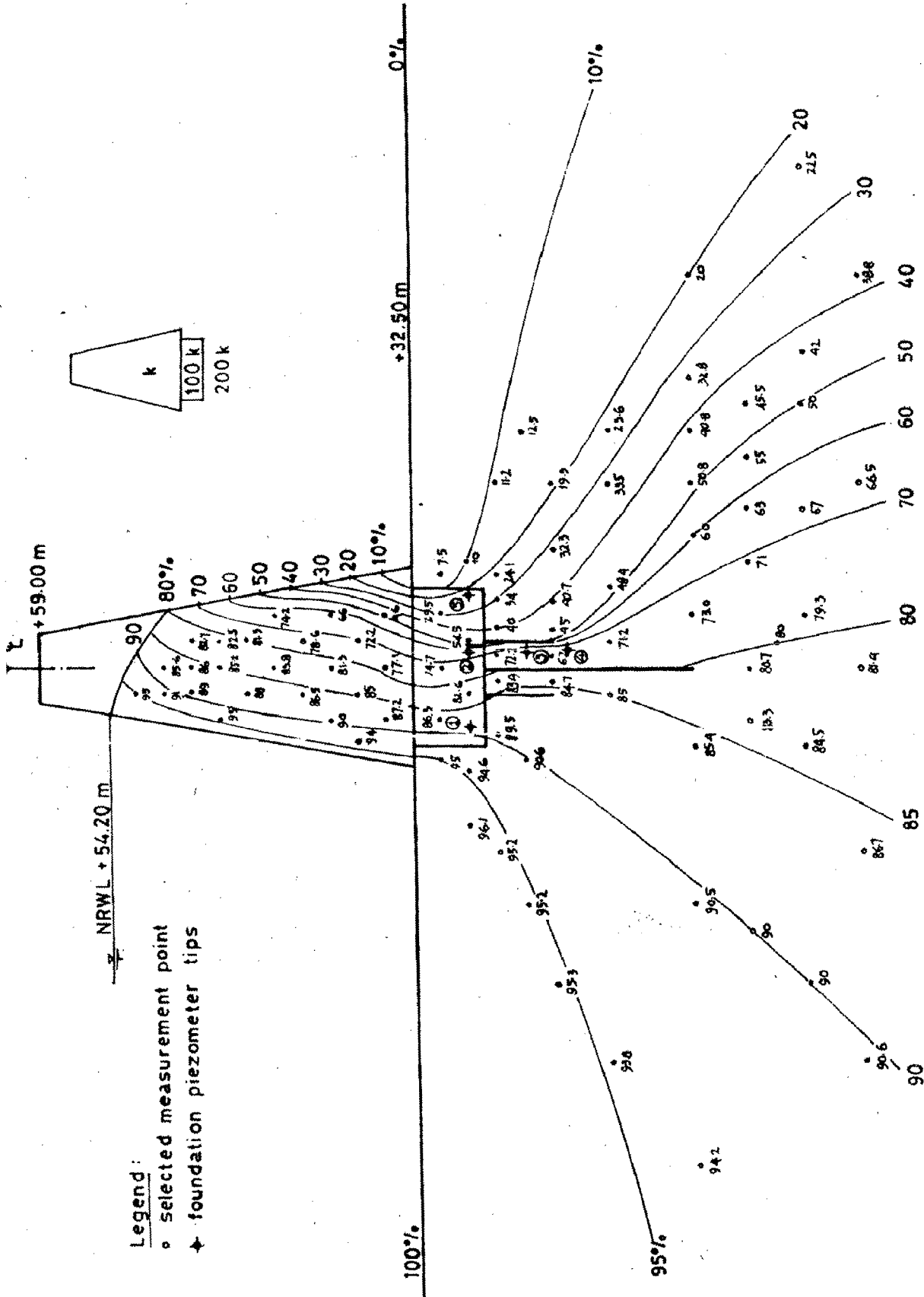


Fig.5.1^b EQUIPOTENTIAL LINES FOR 75% EFFICIENCY OF GROUTS

scale 1:400

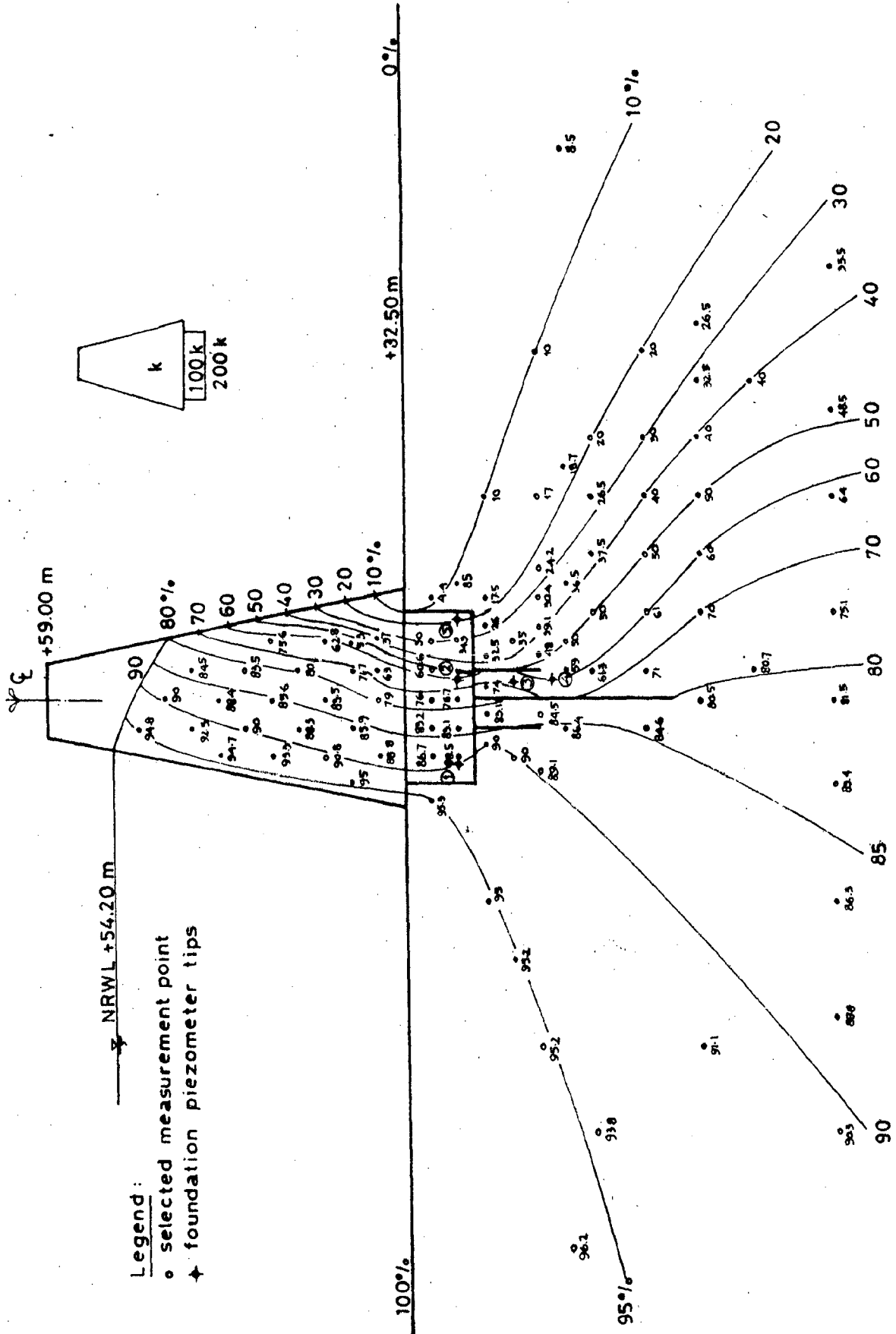


Fig. 5.19 EQUIPOTENTIAL LINES FOR 50% EFFICIENCY OF GROUTS

Scale 1:400

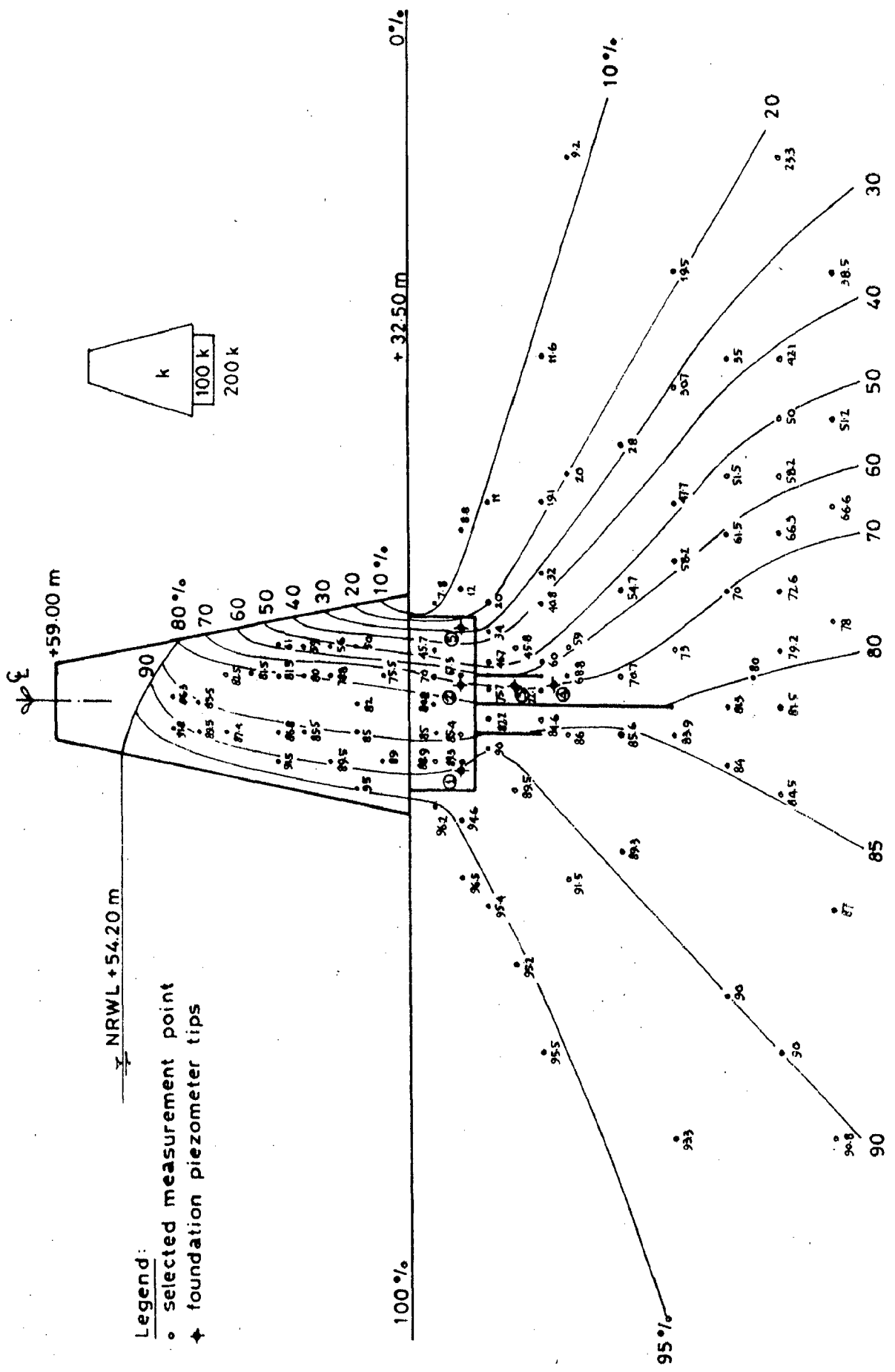


Fig. 5.1d EQUIPOTENTIAL LINES FOR 25% EFFICIENCY OF GROUTS

scale 1:400

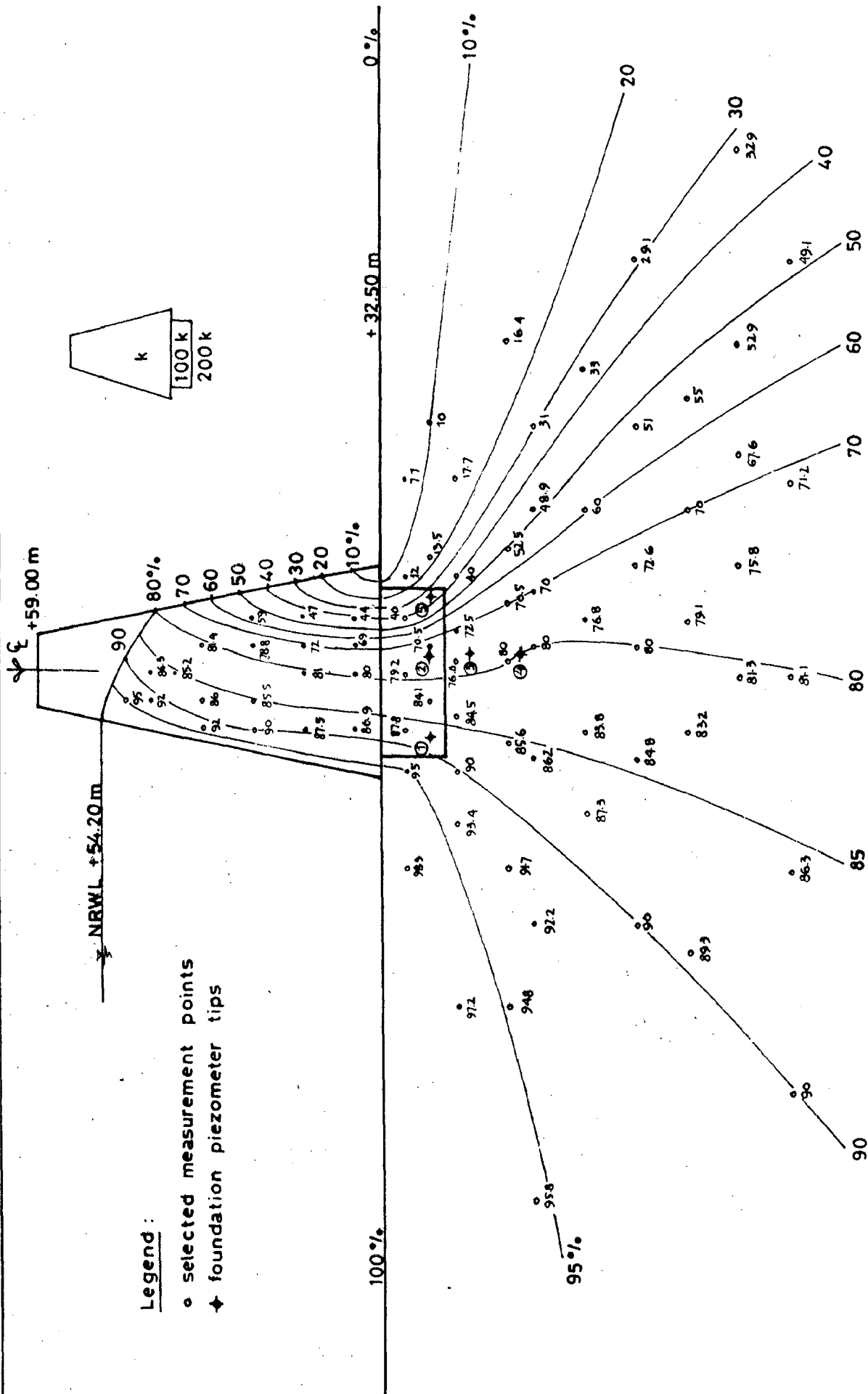
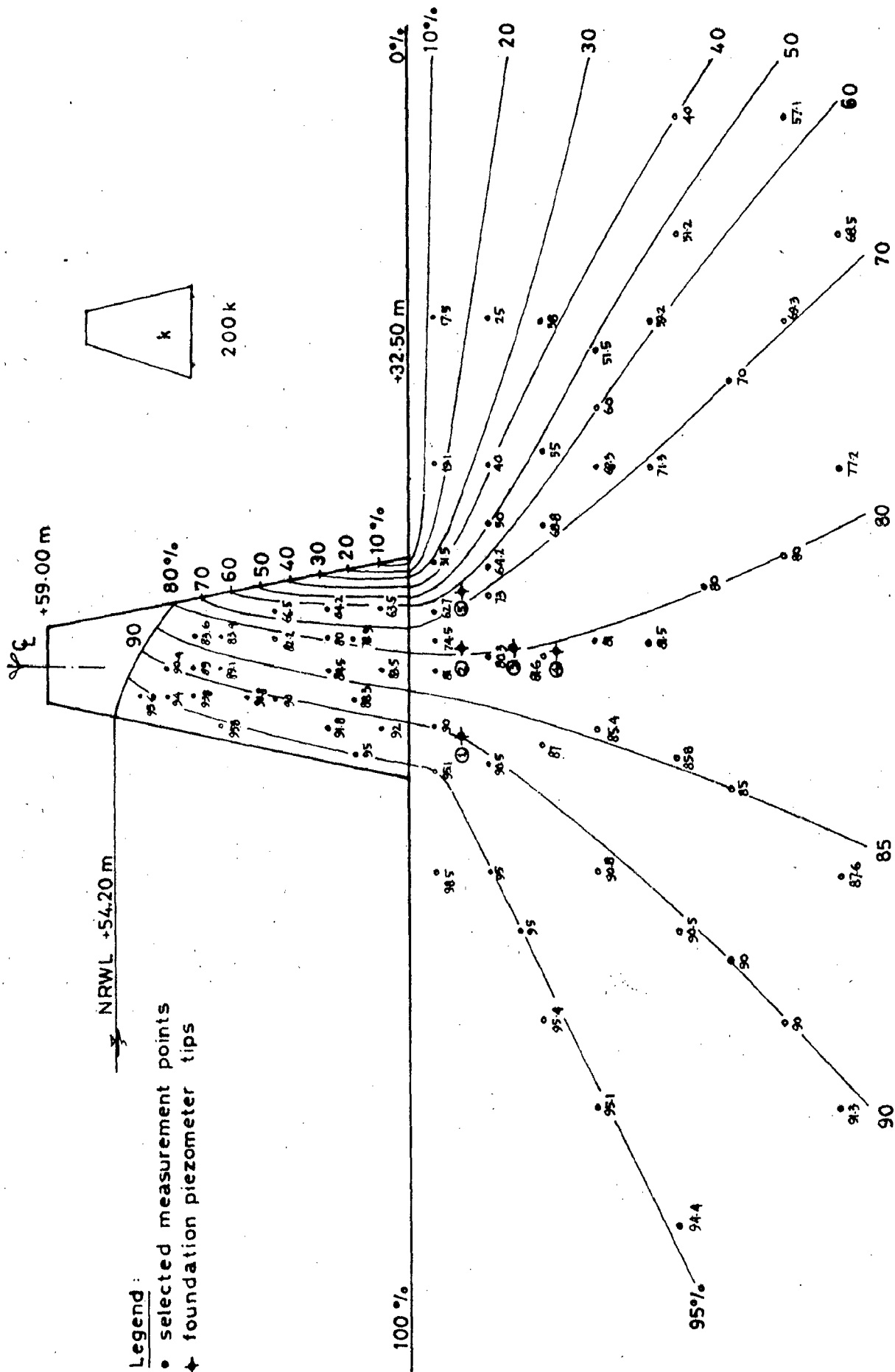


Fig. 5.1^o EQUIPOTENTIAL LINES FOR NO CURTAIN GROUT CONDITION

scale 1:400



Legend:
 • selected measurement points
 + foundation piezometer tips

Fig. 5.1. EQUIPOTENTIAL LINES FOR NO CONSOLIDATION AND CURTAIN GROUTS
 scale 1 : 400

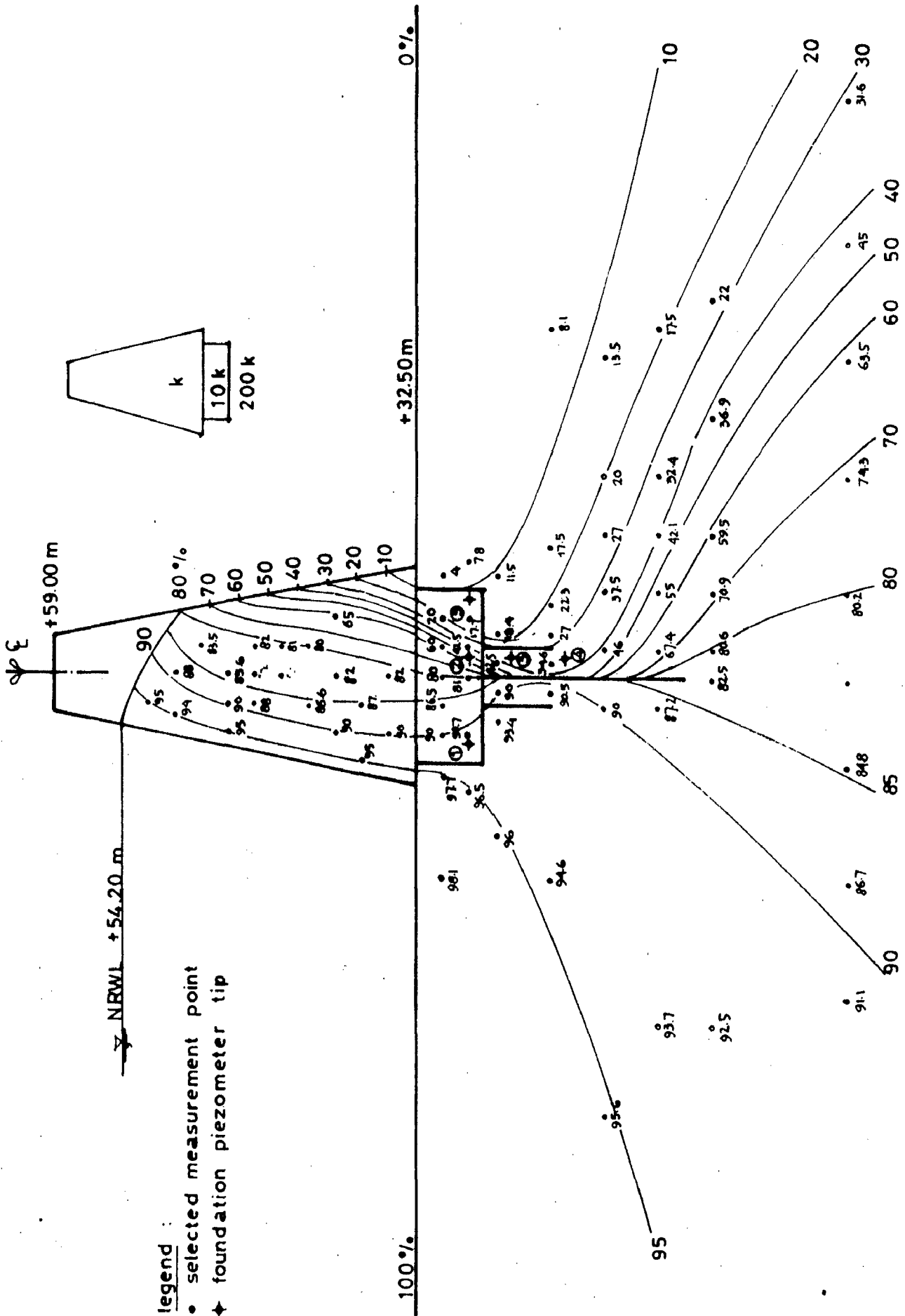


Fig. 5.19 EQUIPOTENTIAL LINES FOR 100% EFFICIENCY OF GROUTS
scale 1:400

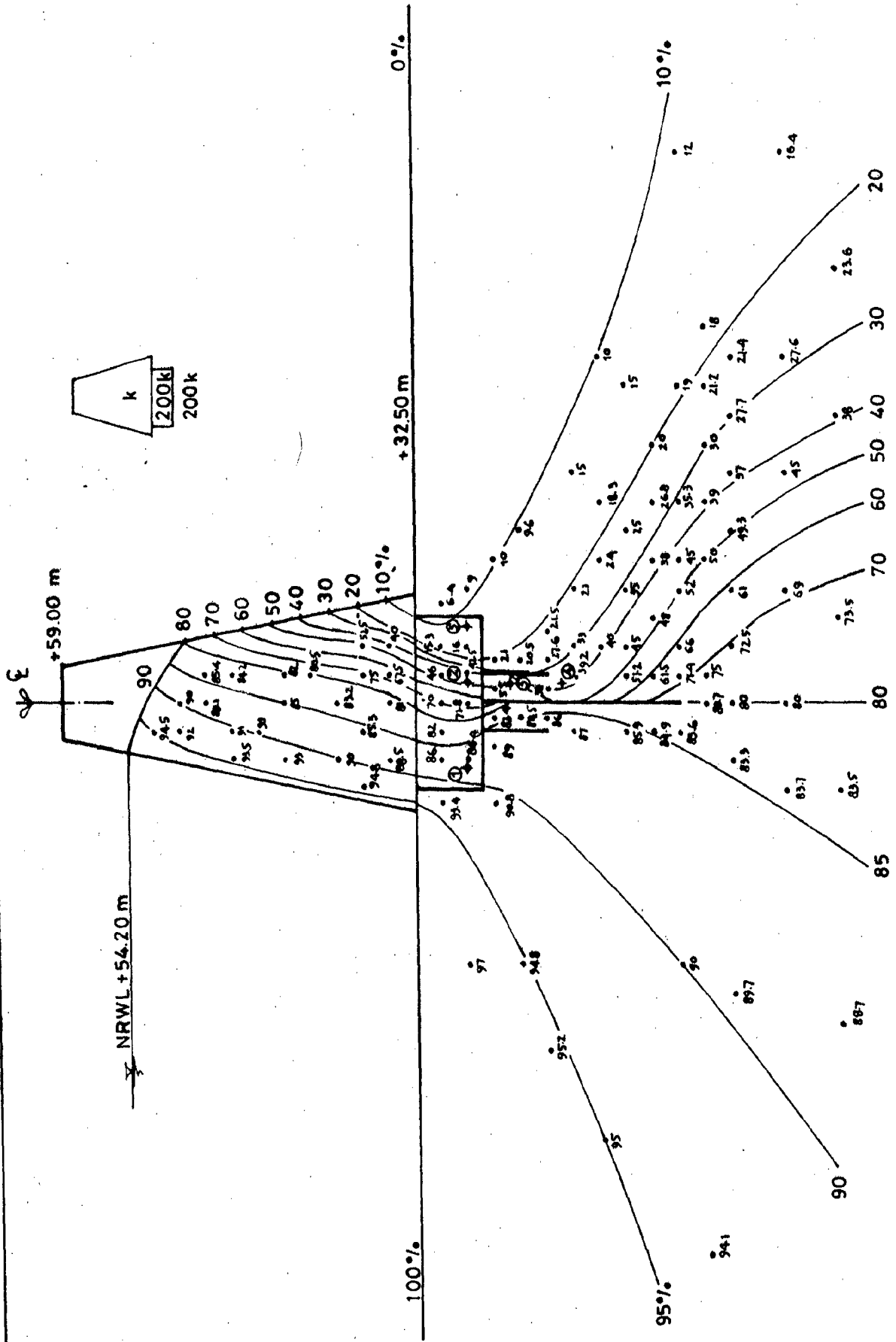


Fig. 51. EQUIPOTENTIAL LINES FOR 100% EFFICIENCY OF GROUTS

scale 1:400

Relative K	Beginning of test		End of test		Remarks	
	Time	Conductivity (μmhs)	Time	Conductivity (μmhs)		
4	5	6	7	8	9	
S	K	9.35AM	5x10 ²	1.08PM	5.4x10 ²	no perforation
		9.45	5x10 ⁴	1.12	4.8x10 ⁴	in the simulated
		10.05	9.95x10 ⁴	1.15	9.8x10 ⁴	grout plastics
		10.10	14.50x10 ⁴	1.20	14.5x10 ⁴	
S	K	9.30AM	4.8x10 ²	12.04	5.0x10 ⁴	25 percent perforation
		9.38	50x10 ⁴	12.10	4.95x10 ⁴	
		9.41	10x10 ⁴	12.15	10.5x10 ⁴	
		9.43	14.5x10 ⁴	12.20	15 x10 ⁴	
S	K	10.05AM	4.85x10 ²	12.10	5.3x10 ²	50 percent perforation
		10.08	5 x10 ⁴	12.15	5 x 10 ⁴	
		10.10	10x10 ⁴	12.18	10 x10 ⁴	
		10.15	19.5x10 ⁴	12.23	14.8x10 ⁴	
S	K	09.45AM	5 x 10 ²	11.40AM	5.25x10 ²	75 percent perforation
		09.47	5 x10 ⁴	11.48	4.95x10 ⁴	
		09.55	10x10 ⁴	11.52	10x10 ⁴	
		09.58	14.5x10 ⁴	11.58	14.5x10 ⁴	

Contd.

Table 5.1(contd.)

1	2	3	4	5	6	7	8	9
31 Oct. '86	0	Core	K	3.15PM	4.95×10^2	4.33PM	5.3×10^2	No curtain
		Grouts	100K	3.17	5×10^4	4.38	5×10^4	grouts
		Found	200K	3.20	10×10^4	4.40	10×10^4	
		Filter	300K	3.23	14.5×10^4	4.50	15×10^4	
4 Nov. '86	0	Core	K	10.07AM	4.95×10^2	12.15	5.3×10^2	No consol. and cur-
		Found	200K	10.10	10×10^4	12.17	10×10^4	tain grouts
		Filter	300K	10.12	14.5×10^4	12.18	14.5×10^4	

Table 5.2 :

Sl. No.	Piez. No.	Elevation	Observed Pore Press. to March '85	Percentage pore pressure from model experiments						
				100% eff.	75% eff.	50% eff.	25% eff.	0% eff.	0% eff. (no curtain)	no consol
1.	FHP 1	15.6	51	90	89	90	90	88	89	
2.	FHP 2	+28.00	12.0	35	55	60	70	74	79	
3.	FHP 5	11.0	30	15	17	20	25	36	65	
4.	FHP 3	+25.00	16.8	43	45	65	70	76	80	
5.	FHP 4	+21.00	24.0	53	46	60	70	80	82	

Note: The relative permeability for clay core zone, consolidation grout zone and foundation zone are K, 100 K and 200 K respectively.

It can be seen from this figure that the grout zone where the piezometers no. FHP1, FHP2 and FHP3 were located are functioning very well, having 100 percent efficiency. But in the consolidation grout zone where piezometer no. FHP 5 was embedded showing the unsuccessful performance of the grout with 21 percent efficiency only. Otherwise in the grout zone of FHP 4 indicating the effect of the grouts having 89 percent efficiency.

A study of Table 5.2 indicates that the percentage pore pressures of FHP1 located at el. + 2800 m from model are almost constant for various cases of efficiencies of grout curtain studied and are of the order of 90 percent, even either in case of no consolidation grout or entire grouts completely ineffective, while observed pore pressure in field is only 51 percent. This observed value seems too low and is not explainable even by model test results. Recording of low values may be either due to malfunction of tip or due to creation of somewhat impervious zone due to grouting around the tip. Observed pore pressure of FHP2 located downstream of grout curtain is of the order of 35 percent whereas those observed on model varying from 55 percent to 79 percent. The pore pressures as observed in the model are increasing as the efficiency of grout curtain is increasing. Reasons for low observed pore pressures recorded by tip no. FHP2 may be the same as for tip no. FHP1. It seems that consolidation grouting is very effective below dam core. Observed pore pressure of piezometer

tip no. FHP5 located at the same elevation (+28.00 m) as that of tip no. FHP1 and FHP2 is of the order of 30 percent where as those observed on model vary from 15 percent to 65 percent. If it is pressured that actual field observation is correct, one may conclude that the curtain grout is efficient only to the extent of about 21 percent (Fig.5.2). Another reason for high observed pore pressures in this tip may be poor quality of consolidation grouting in this region. Permeability of foundation varies from 7×10^{-5} cm/sec to 0.84×10^{-3} cm/sec and the assumption of average permeability of consolidated area as 6×10^{-4} cm/sec. (or 100 K) uniformly throughout may not be correct.

To explore this matter further, model studies were extended with relative permeability of 10K, 50K, 100K and 200 K in consolidation grout zone as well for 100 percent grout curtain efficiency and the results of these studies are shown in Table 5.3.

Table 5.3 - Model Test Results with Variable Permeabilities in Consolidation Zone

Sl. No.	Elev. (m)	Piez. No.	Pore pressure of rel. permeability of consol. grout zone(percent)				Observed pore pressure (percent)
			10K	50K	100K	200 K	
1		FHP1	91	91	90	87	51
2	+28.00	FHP2	50	54	55	50	35
3		FHP5	14	14	15	13	30
4	+28.00	FHP3	37	42	45	39	43
5	+21.00	FHP4	36	38	46	35	53

From this table, it can be seen that percentage pore pressures all the tips are practically of the same order for different permeabilities in consolidation grout zone indicating thereby if permeability in consolidation zone is taken uniform, by and large, there is no significant change in pore pressures recorded by foundation piezometers.

Percentage pore pressure measured by piezometer tip no. FHP3 from model increases from 45 to 80 percent as the grout curtain efficiency decreases whereas observed pore pressure is 43 percent. Thus it can be said that efficiency of grout curtain is almost 100 percent. Similarly, percentage of pore pressure measured by FHP 4 (located also in the downstream of grout curtain at el. + 21.00 m) from model increases from 46 to 32 percent with decreasing efficiency of grout curtain. Observed pore pressure is 53 percent which corresponds to 89 percent efficiency of curtain grout (Fig.5.2).

Thus keeping in view the readings recorded by tips no. FHP1, FHP2, FHP3 and FHP4, it can be said that both grouting viz. consolidation and curtain are by and large successful at this project.

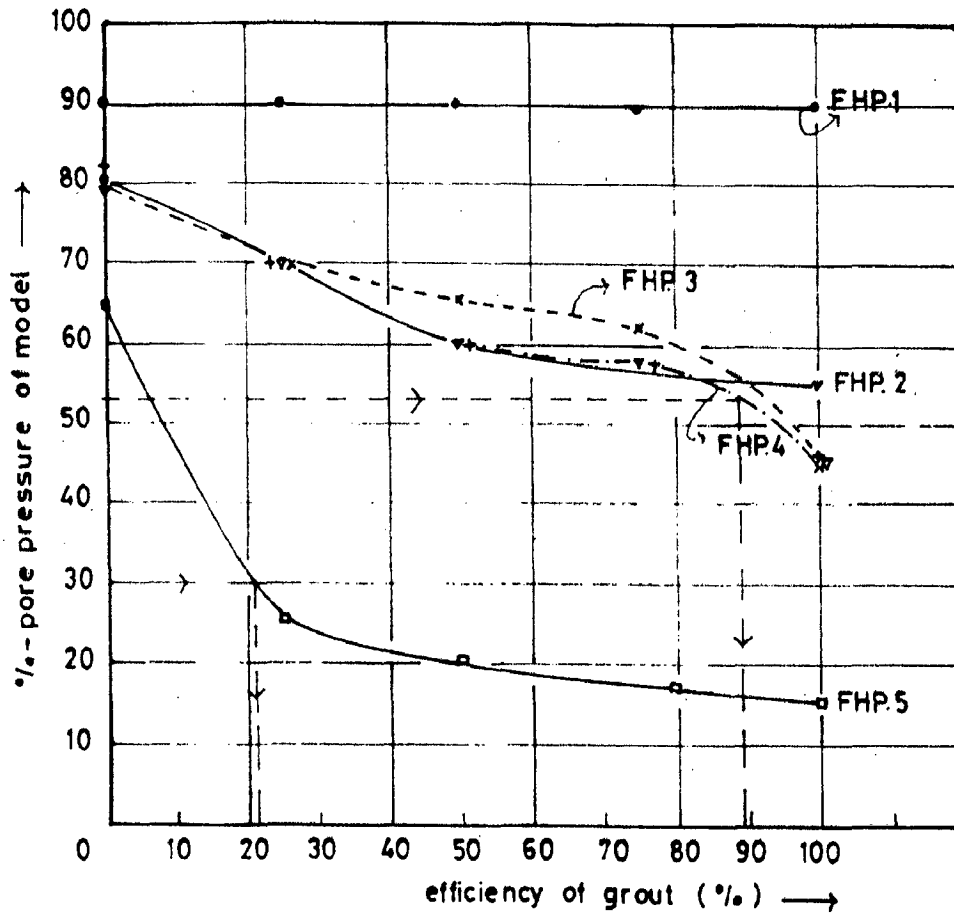


Fig. 5.2. GROUT EFFICIENCY VS. %- PORE PRESSURE

6. CONCLUSION

Following are the brought conclusion :

- 6.1 Twenty eight metres high Rarem Dam section comprises clay core of high plasticity (P.I. about 48%) and rock shells zone having in between transition zone. The dam is resting as permeable tuff rock foundation - the permeability of which of the order of 7×10^{-5} cm/sec to 9.84×10^{-3} cm/sec. Below the dam core, consolidation as well as curtain grouting has been provided. Consolidation grouting has reduced the permeability of foundation to half.
- 6.2 The construction of dam was started at the end of November 1981 and was completed at the beginning of October, 1983. The reservoir filling started in the middle of October 1983 and completed at the beginning of January 1984. There has been no drawdown from the date of filling of reservoir till to date.
- 6.3 Rarem Dam has been instrumented for pore pressures measurement, vertical settlement and horizontal movement.
- 6.4 Twenty seven numbers electrical piezometers were installed but they have not functioned satisfactory.

6.5 Twin tube hydraulic piezometer was installed at Sta. 23⁺¹⁵, total numbers of hydraulic piezometer was 27. A study of the pore pressures data collected from August 1982 till December 1985 has indicated the following :

6.5.1 Construction pore pressures

Where a low construction pore pressures were recorded on this work of the order of 25% of total stress. For clay belonging to CH-group and a very rapid rate of construction, the pore pressures recorded are very low. This may be due to placement of fill dry of OMC (-15%). The density of placement (1.12 t/m^3) is also very low and due to low densities, fill might not behaving as compressible fill.

6.5.2 Steady seepage pore pressures

Data of hydraulic piezometer have shown that the **free** surface line has fully developed. The development of steady seepage pore pressures is practically simultaneous with reservoir filling and there is no time lag. This further shows that the clay core is behaving as incompressible pervious material. Free surface line determined by electrical analogy method is almost the same as that observed from hydraulic piezometer.

6.5.3 Uplift pressures

Piezometer tips embedded in foundation have shown lesser pore pressure than anticipated from theoretical consideration.

6.6 Model study were carried out using electrical analogy method simulating the anisotropy of permeabilities of clay core, consolidation zone, foundation, filters zone and variable efficiencies of grouting. The study have indicated that the grouting done at Rarem Dam is effective.

6.7 Vertical settlement was recorded from August 1982 to October 1985 using magnetic ring type settlement device installed at Sta. 23⁺¹⁰ in the middle of clay core. It has been found that the total settlement is of the order of 30 cm which is almost 50% of the anticipated settlement. It is also seen that the vertical settlement is taking place almost simultaneously with the construction of dam and with the reservoir filling. Very little time lag is observed in settlement. No further settlement is expected in future.

6.8 Horizontal movement

The observations available that in direction perpendicular to dam axis, there is practically no little movement. Whatever initial movement was there during

reservoir filling, the same has been recovered back. However, there is some evident of little movement along the dam axis toward diversion canal side as recorded by the inclinometer installed in lower zone of dam height. These needs further investigation.

REFERENCES

1. Amaya F., Cubillos A and Sierra J.M., ' Pore Pressure Measurements in the Core of Chivar Dam', Proceeding of 10th Inter. Conf. of SMFE, Vol.I, Stockhlom, 1981.
2. Basa, J.P., ' Estimation of Dissipation of Construction Pore Pressure during Construction', M.E. Dissertation in WRDTC, Univ. of Roorkee, 1979.
3. Bishop, A.W., ' Pore Pressure Measurements in the Field and Laboratory', Proceeding of the 7th Inter. Conf. on SMFE, Mexico, 1969.
4. Cedergren, H.R., ' Seepage, Drainage and Flow Nets', John Wiley and Sons Inc. Publication, 1968.
5. Craig, R.F., ' Soil Mechanics', Van Nostrand Reinhold, (U.K.), 1982.
6. Goel, M.C., ' Drawdown Pore Pressures in Earth Dams', Smt. Laxmi Goel, Dehradun, 1986.
7. Hanna, T.H., ' Foundation Instrumentation', Trans Tech. Publications, Ohio, USA, 1973.
8. Hari Krishna and Goel, M.C., ' Pore Pressure Observations and Efficiency of Cut-off Walls at Obra Dam'. Indian Geotechnical Journal, Vol.8, No.3, July 1978.
9. Jeebala Rao, D. and Kurma Rao, K., ' Movement in Some Earth dams during and after Construction', Proceeding on the Symposium on Earth and Rockfill Dams, Punjab, 1968.

10. Little, A.L. and Vail, A.J., ' Some Developments in the Measurement of Pore Pressure', Conf. of the SMFE on Pore Pressure and Suction in Soils, Butterworths, 1961.
11. Mandasia, A.B., ' Optimum Depth of Partial Cut-off with impervious blanket - A Case Study', M.E. Dissertation in WRDTC, Univ. of Roorkee, 1984.
12. Manglik, V.M. and Gupta, R.C., ' Pore Pressures and Displacements in Ramganga Dam', Indian Geotechnical Journal, Vol.7, No.2, April 1977.
13. Penman, AD.M., ' Effect of the Position of the Core on the Behaviour of two rockfill dams', 11th Congress on Large Dam, Madrid, 1973.
14. Radley Squier, L. ' Load transfer in Earth and Rockfill Dams', Journal of SMFE, Vol.96, No.SM1, Jan. 1970.
15. Sherard, J.L., Woodward, R.J. Gizienski, S.F. and Clevenger, W.A. ' Earth-Rockfill Dams', John Wiley and Sons, Inc., New York, 1963.
16. Singh Alam, ' Geotechnical Testing and Instrumentation', Asia Publishing House, 1981.
17. Singh, Bharat and Sharma, H.D., ' Earth and Rockfill Dams', Sarita Prakashan, Meerut, 1976.
18. Singh, Vijendra, ' Determination of Construction Pore Pressures in Compressible Earth Dams', P.G. Dissertation in Department of Mathematics, Univ. of Roorkee, 1985.

19. Tatang Sutardjo and Masngud, ' Hasil pengamatan instrumentasi Geoteknik Bendungan Way-Rarem, Lampung Utara', 3rd Indonesian Conf. on Geotechnical Engineering, Jakarta, 1985.
20. Terzaghi, K and Peck, F.B., ' Soil Mechanics in Engineering Practice', John Wiley and Sons Inc., New York, 1967.